Downregulation of a cell polarity protein potentiates Chikungunya Virus infection in host cells

Pushkar Tatiya[1#,] Ramesh Kumar[1$#,] Debajit Dey[1^], Yashika Ratra[2], Syed Yusuf Mian[2&], Subhomoi Borkotoky[1], Bhawna[2] , Sanchi Arora[2], Kirti Suhag[1], Soumen Basak[2], Manidipa Banerjee[1*]

[1] Kusuma School of Biological Sciences, Indian Institute of Technology Delhi, Hauz Khas, New Delhi
[2] Signaling Systems Laboratory, National Institute of Immunology, Aruna Asaf Ali Marg, New Delhi
[$] Department of Chemistry and Biochemistry, University of Maryland, College Park
^ Current address: Department of Biology, University of York
[&] Department of Immunology and Infectious Diseases, Harvard T.H. Chan School of Public Health

# Equal contribution

*Correspondence: mbanerjee@bioschool.iitd.ac.in

Abstract

Viral manipulation of host cell morphology and behaviour represents an adaptive strategy that increases pathogen survival and replication efficiency. We establish a critical role for the downregulation of human Scribble, part of a cell polarity complex controlling morphology, apoptosis, and migration, for the potentiation of Chikungunya Virus (CHIKV) infection. A structural protein component (TF) of CHIKV targets Scribble, resulting in its punctation, ubiquitination, and subsequent degradation, probably through the proteasome pathway. The interaction between TF and Scribble is mediated *in vivo* by the PDZ domains of Scribble and a PDZ-domain binding motif (PBM) of TF, as shown by a combination of co-localization, co-immunoprecipitation, and proteomics analysis. Disruption of the Scribble polarity protein by shRNA mediated knockdown of Scribble potentiates CHIKV propagation. A mutated version of CHIKV generated through reverse genetics, which produces all structural proteins except TF, cannot affect Scribble to the same extent; and consequently displays reduced infectivity. Our work thus establishes a novel function for the TF component of alphaviruses in the modulation of host response potentiating virus transmission.

Keywords

6K;Chikungunya virus;PDZ domain;Scribble;TF

67 **Introduction**

68 Chikungunya Virus (CHIKV), a member of the alphavirus genus in the *Togaviridae* family, is a
69 mosquito-borne human pathogen that affects almost 100 countries and causes ~3,000,000
70 infections per year globally (Wahid *et al.*, 2017). There are no targeted therapeutics or licensed
71 preventive strategies for CHIKV and the treatment is primarily symptomatic (Bartholomeeusen
72 *et al.*, 2023; Millsapps *et al.*, 2022). While the symptoms caused by this virus are self-limiting,
73 there can be severe complications such as chronic, arthritis-like symptoms; and infections in the
74 very young and elderly populations can be fatal. A clearer understanding of the functionalities of
75 CHIKV encoded proteins, and identification of their host interaction partners, is crucial for the
76 development of targeted therapeutics or attenuated vaccine candidates (Wong & Chu, 2018).

77 The CHIKV capsid, like that of all alphaviruses, is a 60-70 nm particle with T=4 icosahedral
78 geometry (Sun *et al*, 2013; Kielian *et al.,*, 2010; Jose *et al.,*, 2009). The outer layer is composed
79 of 240 heterodimers of envelope glycoproteins E1 and E2, embedded in a host-derived lipid
80 envelope. While E2 is responsible for association with the host cellular receptor(s), E1
81 orchestrates the fusion of the viral and host lipid membranes (Wong & Chu, 2018). The inner
82 layer of the particle consists of 240 copies of a multifunctional capsid protein (C) which
83 encapsulates the genome (Chmielewski *et al.,*, 2022). Another envelope protein, E3, promotes
84 the association between E1 and E2 during virus assembly (Yap *et al*, 2017).

85 The functionalities of the major structural proteins of CHIKV – E1, E2, E3, and C - are well
86 investigated and established. However, a fifth protein – the small structural peptide "6K",
87 remains relatively less explored (Wong & Chu, 2018). While 6K is categorized as a structural
88 protein, its presence in the CHIKV capsid is yet unconfirmed and its role in the virus life cycle
89 remains mysterious. It has been shown that recombinantly generated alphavirus 6K is an ion
90 channel-forming protein (Dey *et al.*, 2019; Melton *et al.*, 2002). The 6K component from Ross
91 River Virus (RRV) and Barmah Forest Virus (BFV) forms cation-specific channels in bilayer
92 membranes in electrophysiology experiments (Melton *et al*, 2002). The expression of 6K in
93 bacterial cells is detrimental to the growth of the cells, which is consistent with 6K possessing
94 membrane-disrupting activity (Sanz *et al*, 1994; Melton *et al*, 2002). Bacterially produced
95 CHIKV 6K, in conjunction with the expression partner Glutathione-S-transferase (GST), forms
96 heterogeneous pores in the membrane *in vitro* (Dey *et al.*, 2019). *In vitro* liposome disruption
97 experiments as well as cellular overexpression models have shown that CHIKV 6K tends to have

98 a strong affinity towards Endoplasmic Reticulum (ER) membranes and congregates in the ER.
99 CHIKV 6K, as well as Sindbis Virus (SV) 6K, co-localize with the glycoprotein E2. SV 6K co-
100 localizes with E2 in cytopathic vesicles on the way to the plasma membrane, which is the budding
101 site for alphaviruses (Dey *et al*, 2019; Brown *et al*, 2018; Elmasri *et al*, 2022). It has been
102 conjectured that 6K is required to facilitate concurrent transport of viral protein and genomic
103 complexes and promote association of glycoproteins during assembly, although there is no clear
104 connection between this functionality and the ion-channel activity of 6K at present.
105 The role of 6K in the alphavirus life cycle has been further complicated by the discovery of a
106 transframe variant "TF", which is generated due to ribosomal slippage within the 6K gene. TF is
107 produced at a 10-18 % frequency during viral protein translation (Firth *et al.*, 2008; Ramsey *et*
108 *al.*, 2019) and shares the majority of the primary amino acid sequence with 6K but varies in the
109 C-terminal region. The production of TF results in premature termination of structural
110 polyprotein translation; thus, E1 is not generated along with TF (Figure 1A). Post-translational
111 modification, specifically palmitoylation, of the Sindbis Virus (SV) TF, is necessary for its
112 association with the plasma membrane (Ramsey *et al.*, 2017). Alphavirus capsids may contain
113 TF as a structural component, albeit in substoichiometric quantities (Snyder *et al.*, 2013; Firth *et*
114 *al.*, 2008). The exact functionality of TF during alphavirus infections is not established; and it
115 remains a mysterious entity like 6K. The functionalities attributed to 6K in many previous works
116 may have been, to some limited extent, influenced by the coexistence of hybrid peptides
117 containing partial sections of TF, due to the non-removal of the ribosomal slippage site within
118 the 6K genomic sequence (Dey *et al.*, 2019;Ramsey & Mukhopadhyay, 2017).
119 Upon a close examination of the CHIKV TF amino acid sequence, we noted that the unique
120 region corresponding to the C-terminal region of TF contains a classical PDZ-domain binding
121 motif (PBM) (Figure 1B). The acronym PDZ originates from the first three proteins discovered
122 to contain this domain – the postsynaptic density protein 95 (PSD95), Drosophila disc large
123 tumour suppressor (Dlg1), and zonula occludens-1 protein (ZO-1) (Ye & Zhang, 2013; Barreda
124 *et al.*, 2018). PDZ domains are protein-protein interaction domains found in practically all life
125 forms. *In silico* docking and simulation studies with the PBM at the C-terminus of TF suggested
126 that a potential binding partner for this motif is Scribble, part of a conserved set of proteins that
127 controls apico-basal as well as planar cell polarities and is also involved in the modulation of
128 tissue morphogenesis and apoptosis (Zhan *et al.*, 2008) (Thomas & Banks, 2018) (Figure 1B).

129 Previous studies have shown that Scribble is targeted by non-structural proteins from Influenza
130 Virus, Human T lymphotropic Virus-1 (HTLV-1), and Hepatitis C Virus (Javorsky *et al.*, 2023);
131 however, the involvement of Scribble in cellular infections by CHIKV or any other alphavirus is
132 so far unknown. In this study, we report that CHIKV infection results in more than 90%
133 abrogation of Scribble protein. Scribble is ubiquitinated and marked for degradation within 24
134 hours of CHIKV infection in HEK293T cells *in vitro*. We present evidence for the involvement
135 of TF in Scribble degradation, as transfection of TF or its production during CHIKV infection
136 results in the sequestration of Scribble into discrete cytosolic puncta. TF also colocalizes in these
137 puncta and can be immunoprecipitated with Scribble during CHIKV infection. The co-
138 localization as well as pulldown of TF with Scribble can be abrogated by mutations within the
139 PBM of TF, showing that the interaction between TF and Scribble is mediated by a PDZ-PBM
140 association. The knockdown of Scribble results in a significant enhancement in CHIKV
141 infectivity in cells. TF-mediated sequestration of Scribble accelerates virus propagation,
142 probably through negative regulation of cellular polarity and pro-apoptotic pathways controlled
143 by the Scribble complex. A version of CHIKV generated through reverse genetics, that does not
144 produce TF, has reduced ability to engage with Scribble and is inhibited in its propagation. Taken
145 together, our data attributes important functions in the contexts of host response modulation and
146 virus propagation to the enigmatic TF component of alphaviruses.
147
148
149

150 **Results**

151 **The unique C-terminus of CHIKV TF contains a PDZ domain binding motif with potential**
152 **for association with Scribble**

153 The first 49 amino acids in the protein sequence of CHIKV 6K and TF are identical. This region
154 is highly hydrophobic and capable of lipid membrane interaction as shown before (Dey *et al.*,
155 2019; Firth *et al.*, 2008). A ribosomal 212-1 frameshift at a slippery sequence corresponding to
156 residues 48-49 within the 6K gene results in the production of TF with a unique C-terminal region
157 of 27 amino acid residues which is primarily hydrophilic (Figure 1A). A motif search of this
158 region indicated the presence of a putative PBM at the extreme C-terminus (Figure 1B). The
159 Eukaryotic Linear Motif (ELM) resource (Kumar *et al.*, 2022) predicted that TF residues 71-76,
160 with the sequence HGGSTV, constitute a class I PBM. This was confirmed by PDZPepInt, a
161 PDZ domain identification software (Kundu *et al.*, 2014; Kundu & Backofen, 2014), which
162 further predicted that residues 71-75 (HGGST) can constitute a potential binding motif for the
163 host protein Scribble. Mammalian Scribble, a cell polarity component with four PDZ domains,
164 is targeted by multiple viral proteins through PDZ-PBM interactions (Javorsky *et al.*, 2023).
165 Particularly, domains 1 and 4 of Scribble have previously been reported to be high-affinity
166 binders (Janezic *et al.*, 2019). We attempted to check the association of CHIKV TF with the PDZ
167 binding domains of Scribble using *in silico* methods. A predicted structure of full-length TF
168 (from the I-TASSER web server) was docked against PDZ domains 1, 2, 3, and 4 of Scribble
169 (designated ScPDZ1, ScPDZ2, ScPDZ3, and ScPDZ4) using the ClusPro web server. The best-
170 scoring models were selected for further analysis, and the binding interface was analyzed using
171 Ligplot (Figure 1C, Supplementary Figure S1). MD simulations of TF in conjunction with
172 ScPDZ1, ScPDZ2, ScPDZ3, and ScPDZ4 were subsequently carried out. In order to determine
173 whether the interaction with the PBM of CHIKV TF is specific to the PDZ domains of Scribble,
174 a PDZ domain from the mammalian High-temperature requirement A1 enzyme, a serine protease
175 (HtrA1) (Wang & Nie, 2021) was also included in the study as a control. Several residues at the
176 C-terminus of TF were found to be involved in mediating hydrogen bonds and hydrophobic
177 interactions with residues of the PDZ domains 1 and 4 of Scribble (Table 1). An RMSF plot
178 (Figure 1D) and RMSD (Supplementary Figure S2) analysis of the simulation trajectory showed
179 that TF was stabilized by the Scribble PDZ domains. In particular, local fluctuations in the C-
180 terminal tail of TF were significantly reduced upon interaction with ScPDZ1 (Figure 1D). These

181 fluctuations were most pronounced in simulations of TF alone. However, HtrA1 PDZ interaction
182 had minimal effect on the TF C-tail fluctuations (Figure 1D). Higher binding energies were
183 observed for the interaction of TF with the PDZ domains of Scribble in contrast to that of HtrA1
184 (ScPDZ1>ScPDZ4>>HtPDZ) (Supplementary Table S1). Specifically, TF-HtPDZ interaction
185 was observed to be ~3.8 times weaker than that with ScPDZ4 and ~5.8 times weaker as compared
186 to TF-ScPDZ1. The binding energies in all cases were primarily mediated by electrostatic and
187 van der Waals interactions (Figure 1C, Supplementary Table S1). Thus, *in silico* analysis
188 indicated that CHIKV TF preferentially binds to the PDZ domains 1 and 4 of Scribble, as
189 compared to PDZ domains from other mammalian proteins. The association of TF with ScPDZ2
190 and ScPDZ3 was also analyzed (Supplementary Figure S1), and the binding energies were found
191 to be at least 2-fold lower than that of TF-ScPDZ1 and 1.4 times lower than that of TF-ScPDZ4
192 (Supplementary Table S1). Further analysis of the TF interface residues with ScPDZ1 (Figure
193 1E) revealed that several C-terminal residues of TF, which are part of the putative PDZ-domain
194 binding motif, contributed favourably towards binding with ScPDZ1.
195
196 **Overexpressed CHIKV TF co-localizes with Scribble**
197 In order to investigate interactions between TF and Scribble biochemically, a plasmid containing
198 the cDNA of CHIKV TF, with an N-terminal Enhanced Green Fluorescent Protein (EGFP) tag
199 (EGFP-TF), was transfected in HEK293T cells. To check for the specificity of the putative
200 interaction, the cDNA of CHIKV 6K, which shares the N-terminal forty-nine residues with TF,
201 was similarly fused with EGFP to form EGFP-6K and transfected. The ribosomal slippage site
202 was mutated in the 6K construct to prevent the initiation of TF expression from this plasmid
203 (Supplementary Table S2). Twenty-four hours post-transfection, cells were fixed and immuno-
204 stained with a Scribble-specific antibody to establish the intracellular localization of Scribble in
205 the presence of CHIKV TF or 6K (Figure 2A). In mock-transfected cells, Scribble was found to
206 localize primarily to the cellular periphery near the plasma membrane. Similarly, Scribble
207 localized to the plasma membrane in cells transfected with an empty vector (pEGFPC1), and no
208 co-localization with EGFP was noted (Figure 2A). However, in cells transfected with EGFP-TF,
209 the localization of Scribble was drastically altered. In these cells, EGFP-TF and Scribble were
210 found to co-localize in the form of distinct puncta in the cytoplasm (Figure 2A). No such co-
211 localization was noted upon transfection of cells with EGFP-6K. In order to establish co-

212 localization in a semi-quantitative fashion, we utilized intensity line profile analysis. The profile
213 graph displays the fluorescence signal intensity along the y-axis and the position or distance along
214 the x-axis for two fluorochromes. The overlapping intensity peaks clearly suggested that while
215 there is limited co-localization between 6K and Scribble, the co-localization between TF and
216 Scribble is substantial (Figure 2A and Supplementary Figure S3). We hypothesized that the
217 prominent punctation and mis-localization of Scribble is probably mediated by the unique C-
218 terminal region of TF, since the N-terminal regions of 6K and TF are identical (Figure 1A).
219 Given the conclusions of the *in-silico* studies, we further hypothesized that the association
220 between Scribble and TF is likely mediated by the PDZ domain(s) and PDZ-binding motifs of
221 the components.

222 **The interaction between TF and Scribble is mediated by a PDZ-PBM interaction**

223 In order to investigate the association between TF and Scribble, the putative PBM in CHIKV TF
224 (71-HGGSTV-76) was mutated to contain either two or four alanine substitutions
225 (HGAATV/AAAATV). The constructs were designated TF Mut1 and TF Mut 2, respectively.
226 The corresponding plasmids with the mutated EGFP-TF sequences were individually transfected
227 in HEK293T cells, and the effect of these mutants on Scribble localization was analyzed using
228 confocal microscopy.

229 We did not observe puncta formation by Scribble in cells transfected with the mutated EGFP-TF
230 constructs (Figure 2B). The fluorescence associated with TF Mut1 and TF Mut2 had a strikingly
231 different distribution compared to wildtype TF. No co-localization was detected between
232 Scribble and PBM mutated TF constructs visually and upon semi-quantification via line profile
233 analysis (Figure 2B and Supplementary Figure S3). To confirm that the TF PBM mutants were
234 being expressed in cells, the expression level of wildtype and mutated EGFP-TF constructs were
235 investigated via Western blots (Figure 2C). A slight reduction in the protein expression level of
236 EGFP-TF with the PBM mutated to HGAATV (TF Mut1) compared to wildtype was observed,
237 while the EGFP-TF construct with a quadruple alanine mutation (TF Mut2) displayed further
238 reduced expression. However, the molecular weight difference between EGFP only, EGFP-6K
239 and the EGFP-TF constructs clearly indicated the expression of the correct proteins in transfected
240 cells (Figure 2C). Further, the alteration in the cellular expression pattern of the mutated
241 constructs and the lack of co-localization with Scribble strongly suggested that the putative PDZ
242 binding motif HGGSTV is critical for the association between TF and Scribble (Figure 2A-C).

243 To probe this interaction further, we immunoprecipitated Scribble with a rabbit polyclonal
244 antibody from HEK293T cells transfected with EGFP only, EGFP-TF, EGFP-TFMut1 and
245 EGFP-TFMut2. The immunoprecipitated fractions were probed with an anti-Scribble antibody
246 and an anti-GFP antibody to identify TF and TF mutants (Figure 2D). We found that while EGFP-
247 TF could be immunoprecipitated with an anti-Scribble antibody; EGFP-TFMut1 or EGFP-
248 TFMut2 could not be pulled down along with Scribble. This strongly indicates that the
249 association between Scribble and TF is mediated via the PDZ domains of the former and the
250 PBM of the latter, since mutating the PBM abrogated the association.
251 To establish the differences in Scribble binding by wildtype vs PBM mutated versions of TF,
252 LC-MS/MS analysis of trypsin-digested fragments from the immunoprecipitated fractions was
253 carried out. While wildtype EGFP-TF had a substantial coverage in the fractions
254 immunoprecipitated by an anti-Scribble antibody, EGFP-TF Mut1 and EGFP-TF Mut2 had
255 significantly reduced coverage and fewer peptides, less than half of that observed for the wildtype
256 EGFP-TF (Table 2), suggesting considerably lower association of the mutated versions of TF
257 with Scribble. A list of all the proteins immunoprecipitated is shown in the supplementary file
258 (MS ANALYSIS). Taken together, co-localization studies, immunoprecipitation, and mass
259 spectrometry clearly establish that the *in vivo* association between Scribble and CHIKV TF is
260 driven by the interaction between the PDZ domain(s) of the former and the PBM at the unique
261 C-terminus of TF.
262
263 **TF associates with Scribble during CHIKV infection:** In order to determine if the association
264 of TF with Scribble has any functional relevance, the interaction was investigated during CHIKV
265 infection of HEK293T cells. An antibody was raised against the unique region of CHIKV TF,
266 by utilizing the C-terminal 27 amino acids coupled with Keyhole Limpet Hemocyanin (KLH) as
267 an antigen. The antibody, generated in rabbit, was tested for its ability to recognize TF in western
268 blots as well as in immunofluorescence assays (Supplementary Figure S4). The association of
269 the antibody with TF was found to be specific as it was able to recognize bacterially produced
270 and purified TF (conjugated with the Maltose Binding Protein, MBP), as well as EGFP-TF from
271 a HEK293T cell lysate, but was unable to bind to bacterially produced MBP-6K or overexpressed
272 EGFP-6K (Supplementary Figure S4).

273 The antibody against TF was utilized to visualize the localization and association of TF during
274 CHIKV infection. Confocal microscopy studies showed substantial production of TF during
275 CHIKV infection of HEK293T cells and significant TF co-localization with Scribble in punctate
276 forms (Figure 3A and Supplementary Figure S5). The co-localization was also validated by
277 intensity line profile analysis (Figure 3A). For comparison, CHIKV capsid protein and
278 glycoprotein E2 were also immunostained using specific antibodies (Figure 3B); however, there
279 was no co-localization of Scribble with either capsid protein C or E2. To understand the dynamics
280 of viral protein production and co-localization, CHIKV-infected cells were probed
281 simultaneously with E2 and Scribble antibodies or E2 and TF antibodies at 24 hours post-
282 infection. Interestingly, while E2 did not co-localize with Scribble even after 24 hours of
283 infection, substantial co-localization was noted between E2 and TF (Figure 3C).
284 The association between Scribble and TF during CHIKV infections was further established by
285 immunoprecipitation of Scribble using a polyclonal anti-Scribble antibody from CHIKV-infected
286 HEK293T cell lysates. Western blotting of the co-IP fractions with the TF unique-region specific
287 antibody clearly indicated the presence of TF (Figure 3D), thus establishing the association of
288 TF with Scribble during CHIKV infection.
289
290 **CHIKV infection, or TF expression, results in degradation of Scribble**
291 Multiple viruses have been shown to target Scribble for degradation in order to manipulate host
292 immune responses, cell junction integrity, and apoptosis pathways (Javorsky *et al.*, 2023). In
293 order to analyze the effect of CHIKV infection on the level of Scribble, the levels of Scribble
294 protein were detected by western blotting in HEK293T cells 24 and 48 h post infection (Figure
295 4A). A significant decrease in Scribble protein level was noted upon CHIKV infection in a time-
296 dependent manner. At 24 hours post-infection, Scribble levels were reduced to nearly 50%
297 compared to uninfected cells. The protein levels reduced to greater than 95% at 48 hpi (Figure
298 4A), while those in uninfected cells remained at the initial level. Thus, CHIKV infection appeared
299 to cause a drastic reduction in the levels of human Scribble protein in cell culture.
300 To confirm that Scribble degradation during CHIKV infection is triggered by the TF component,
301 the effect of overexpressed TF on Scribble protein expression level was also evaluated (Figure
302 4B). Since CHIKV-induced reduction in Scribble protein levels was the highest 48 h post
303 infection, the effect of TF, upon transfection, on Scribble expression was also studied at 48 h.

304 Transfection of HEK293T cells with the EGFP-TF plasmid, containing the wildtype sequence of
305 TF, was found to reduce the level of Scribble protein by ~20%. The higher levels of Scribble
306 degradation in CHIKV-infected versus TF-transfected cells is probably due to the different levels
307 of TF expression in the infection versus the transfection model. The reduction in Scribble protein
308 level was not elicited by transfection of EGFP-6K, or EGFP-TF Mut1 and EGFP-TF Mut2,
309 (Figure 4B), indicating that this effect is triggered by TF, and is specific to the PBM at the C-
310 terminus of TF.
311 The mode of degradation of Scribble was explored by co-staining CHIKV-infected cells with
312 anti-Scribble and anti-Ubiquitin primary antibodies and appropriate secondary antibodies (Figure
313 4C). We found strong co-localization of the Scribble puncta with ubiquitin-specific antibodies in
314 CHIKV-infected HEK293T cells, which suggests that CHIKV-mediated degradation of Scribble
315 could be mediated by the Ubiquitin-Proteasome System (UPS). Similarly, in transfected cells
316 overexpressing TF, co-localization of Scribble, Ubiquitin, and TF was detected in cytoplasmic
317 puncta (Figure 5A). While some Scribble punctation, albeit at a lower level, was noted during
318 overexpression of the double alanine PBM mutant (EGFP-TF-HGAATV), there was no co-
319 localization of ubiquitin to these puncta (Figure 5A).
320 To further investigate the involvement of the UPS in Scribble degradation, ubiquitinated proteins
321 in CHIKV infected or uninfected HEK293T cells were analyzed in the presence of the
322 proteasome inhibitor MG-132 (Figure 5B). In uninfected cells, the addition of MG-132 had no
323 effect on Scribble quantities. However, the addition of MG-132 restored the reduction in Scribble
324 triggered by CHIKV infection.
325 Thus, taken together, our results suggest that during CHIKV infection, the TF component
326 associates with Scribble through its C-terminal PBM (HGGSTV), resulting in the punctation and
327 degradation of Scribble. The alterations in Scribble quantities upon the addition of MG132
328 suggest that the degradation of Scribble probably occurs through the UPS pathway.
329
330 **Scribble knockdown enhances CHIKV infection**
331 In order to investigate the significance of Scribble downregulation during CHIKV infection, the
332 level of CHIKV propagation in Scribble knockdown cells was compared to that in untreated cells.
333 Two short hairpin RNAs (shRNAs) were used for the knockdown of Scribble protein expression
334 in HEK293T cells according to standard protocols. The effect of the shRNAs was analyzed 36

335 hours post-transfection using western blot analysis. Densitometric analysis, to quantitate the
336 relative percentage of gene knockdown for each sample, indicated a relatively efficient Scribble
337 protein knockdown of approximately 50% with both shRNA conditions (Figure 6A) . The degree
338 of knockdown at the RNA level was also confirmed using quantitative real-time polymerase
339 chain reaction (qRT-PCR) (Figure 6B). To ensure that any alteration observed in CHIKV
340 infectivity upon Scribble knockdown was indeed because of a reduction in the quantity of
341 Scribble, and not due to a difference in the number of viable cells as an effect of knockdown, cell
342 viability was assessed using an MTT assay (Figure 6C). No significant change in cell viability
343 was observed with Scribble knockdown.
344 The HEK293T cells with reduced Scribble expression were then infected with CHIKV (strain
345 119067) at an MOI of 0.1. The culture supernatants containing the new virus were harvested 24
346 h post infection and plaque assay was performed using standard methodologies in Vero cells.
347 CHIKV infectivity was calculated by counting the number of plaques formed 48 h post-virus
348 addition. We found that the virus titre, represented as the plaque forming unit per ml (pfu/ml),
349 was significantly increased upon Scribble knockdown (Figure 6D). We also tested the levels of
350 CHIKV RNA in infected HEK293T cells with Scribble knockdown by RT-PCR and found that
351 the levels of CHIKV RNA were also markedly upregulated in these cells, compared to regular
352 infected cells (Figure 6E). The increase in infectious CHIKV virions and genomic RNA was
353 approximately 2-3 times higher upon Scribble knockdown. Taken together, our data strongly
354 suggest that punctation and degradation of Scribble is a viral countermeasure to facilitate CHIKV
355 propagation and is mediated by TF.
356
357 **Infection with ΔTF CHIKV does not trigger Scribble punctation**
358 To further investigate the role of TF during CHIKV infection, a mutated version of CHIKV was
359 generated to produce all structural proteins including 6K, but not TF. An infectious clone of the
360 CHIKV OPY-1 strain with an mCherry cassette for detection (mCherry-LR2006-OPY1)
361 (Hallengärd et al, 2014) was utilized as a template to generate a silent mutation in the ribosomal
362 slippage site, to abrogate the production of TF. Both infectious clones - WT CHIKV and ΔTF
363 CHIKV - were transfected in HEK293T cells using the standard protocol for the formation of
364 virus particles. The transfection supernatants were subjected to plaque assays and the viral
365 plaques in each case were isolated and subjected to serial infections to increase the titre. We

366 confirmed, using specific antibodies, that while infection with WT CHIKV results in the
367 production of TF as well as other structural proteins; infection with ΔTF CHIKV produces 6K,
368 but not TF (Supplementary Figure. S9).
369
370 ΔTF CHIKV at 1 MOI was utilized to infect HEK293T cells, and the WT virus at the same MOI
371 was utilized in control infections. The plaque assay consistently suggested lower cellular
372 infectivity for ΔTF CHIKV compared to WT virus. qRT-PCR based quantification of viral RNA
373 for the WT and ΔTF CHIKV virus showed higher viral RNA load in cells infected with ΔTF
374 CHIKV 12 hpi(Figure 7A). This indicates production of significantly higher numbers of progeny
375 virions that are release/assembly defective when TF is absent. The observation re-emphasizes the
376 critical nature of cell polarity/adhesion disruption mediated by ubiquitination of scribble for
377 CHIKV transmission in vitro. Cells infected with WT or ΔTF CHIKV were co-stained with anti-
378 Scribble and anti-Ubiquitin antibodies to detect the extent of Scribble punctation and ubiquitin
379 co-localization with Scribble (Figure 7B). Scribble appeared prominently in punctate form 24
380 hours post-infection in WT CHIKV-infected cells. Significant co-localization of Scribble and
381 ubiquitin-specific antibodies was observed in WT CHIKV-infected HEK293T cells 12 hours
382 post-infection, intensifying at 24 hours (Figure 7B). In contrast, while ΔTF CHIKV-infected cells
383 did have limited amount of Scribble puncta, these did not co-localize with Ubiquitin (Figure 7B).
384 Since Scribble and Ubiquitin co-localization was observed in WT mCherry-LR2006-OPY1
385 CHIKV 24 hours post-infection, cellular lysates from WT and ΔTF CHIKV OPY-1 infected cells
386 were subjected to western blotting with anti-Scribble antibody at 24 hours p.i and 12 hours post
387 this time point (Figure 7C). A significant, time-dependent, decrease in Scribble protein levels
388 was observed in cells infected with WT CHIKV OPY-1 strain. In contrast, cells infected with
389 ΔTF CHIKV OPY-1 showed Scribble levels slightly above normal (Figure 7C). Together, these
390 results demonstrate that the TF component of CHIKV is crucial for effective ubiquitination and
391 downregulation of Scribble, a process that cannot be executed by ΔTF CHIKV. Thus, the TF
392 component of CHIKV is crucial for downregulating Scribble in infected cells, which enhances
393 viral infectivity and propagation.
394

395 **Discussion**

396 Host-virus interactions play a crucial role in defining the trajectory of pathogenesis
397 (Krishnakumar & Kannan, 2020). Key host molecules and pathways are consistently hijacked by
398 viruses to ensure the propagation of infection. Some widely targeted host cellular co-factors
399 include nuclear pore/envelope complexes, COPI vesicles, ribosomes and the translational
400 pathway and signalling modulators (Ma-Lauer *et al.*, 2012). Increasing evidence suggests that
401 the Scribble cell polarity complex is one of the central host factors targeted by multiple virus
402 families (Javorsky *et al.*, 2023). Human Scribble is part of a large module of adapters, including
403 several Dlg and Lgl proteins, which has a central role in regulating cell migration, adhesion,
404 polarity, signalling, apoptosis, morphogenesis, and development (Bonello & Peifer, 2019;
405 Santoni *et al.*, 2020; Stephens *et al.*, 2018). The members of this complex associate with a wide
406 range of cellular factors to modulate cellular activities. Scribble is a member of the LAP (leucine-
407 rich repeats and PDZ domain) family and contains numerous protein-protein interaction domains,
408 including 16 Leucine-Rich Repeat domains (LRRs), 2 LAP-specific domains, and 4 PDZ
409 domains (PDZ1-4). Loss of Scribble causes disruption of cellular adhesion and cell polarity,
410 resulting in hyperproliferation (Bonello & Peifer, 2019). As a determinant of cellular growth,
411 apoptosis and proliferation, Scribble has been a target of tumorigenic viruses such as Human
412 Papillomavirus (HPV) and Human T-lymphotropic virus 1 (HTLV-1) (Arpin-André & Mesnard,
413 2007; Nakagawa & Huibregtse, 2000). Recently, effectors from several other viruses, such as the
414 NS1 protein from Influenza A Virus (IAV), NS5 from Tick-borne encephalitis virus (TBEV),
415 and the core protein from Hepatitis C Virus (HCV), have been shown to associate with the PDZ
416 domains of Scribble through PBMs, resulting in mistargeting of Scribble and an increase in viral
417 proliferation (Javorsky *et al.*, 2023). However, there have been no reports of Scribble modulation
418 by alphaviruses so far. In this manuscript, we establish Scribble as a host target of CHIKV and
419 identify the viral factor that induces the mislocalization and degradation of Scribble to enhance
420 viral proliferation.

421

422 We found that CHIKV infection downregulates Scribble expression by as much as 95% in
423 cultured cells in a time-dependent manner. Immunofluorescence analysis of CHIKV-infected
424 cells showed clustering of Scribble into cytoplasmic puncta, and ubiquitin-mediated degradation.
425 Degradation of Scribble via the Ubiquitin-Proteasome pathway was suggested by experimental

426 studies using a proteasome inhibitor, MG132. The cellular localization of Scribble is important
427 for its functioning (Javorsky *et al.*, 2023; Zhan *et al.*, 2008; Stephens *et al.*, 2018), and
428 mislocalization of Scribble and its sequestration in discrete puncta likely affect its regulatory role
429 in cellular proliferation (Arpin-André & Mesnard, 2007; Liu *et al.*, 2010). To confirm the role of
430 Scribble in CHIKV infection, shRNA-based downregulation of Scribble expression was carried
431 out. A ~50% downregulation in Scribble levels resulted in 2-3 times increase in the virus titer
432 and genomic RNA levels. This effect may be due to the elimination of the pro-apoptotic activity
433 of Scribble, resulting in prolonged cell survival and consequent enhancement in viral replication
434 (Liu *et al.*, 2010). Scribble is a cell polarity protein that is important for maintaining the integrity
435 of cellular junctions, and disruption of cell junctions has been reported to promote virus egress
436 and dissemination (Javorsky *et al.*, 2023; Bonello & Peifer, 2019; Torres-Flores & Arias, 2015;
437 Thomas & Banks, 2018). While HEK293T cells do not contain conventional tight junctions, they
438 do produce a number of cell adhesion molecules such as E-cadherin, occluding and ZO-1, in
439 addition to Scribble (Inada *et al.,* 2016*)* Thus, the beneficial effect of Scribble knockdown on
440 CHIKV replication might be due to alteration in cellular contacts, allowing enhancement of viral
441 release. A more detailed analysis of the timeline of CHIKV-mediated Scribble downregulation
442 and consequent spatio-temporal effects on cellular morphology, adhesion and signalling may be
443 essential for understanding the functional basis for viral countermeasures to host response.
444
445 The small structural protein 6K, and its transframe variant TF, appear to have significant
446 importance in the regulation of CHIKV morphology and virus-host interactions (Ramsey &
447 Mukhopadhyay, 2017). It has been shown previously that CHIKV 6K, like its homologs from
448 other alphaviruses, is an ion-channel forming protein (Dey *et al.*, 2019). It has been shown that
449 inhibition of 6K activity may affect CHIKV assembly, resulting in the formation of
450 morphologically unusual particles with reduced infectivity. Recent work has shown that 6K co-
451 localizes with alphavirus glycoproteins in cytopathic vesicles (CPV-II), which may support its
452 role in promoting viral assembly (Elmasri *et al.*, 2022). TF, in contrast, localizes at the plasma
453 membrane and is packaged in virions (Firth *et al.*, 2008; Ramsey *et al.*, 2017). Our work attributes
454 an essential role to TF in the modulation of host response and in the enhancement of viral
455 proliferation. Several lines of evidence show that the TF component of CHIKV is primarily
456 responsible for the downregulation of Scribble. The expression of TF in HEK293T cells by

457 transfection leads to the sequestration of Scribble into distinct puncta, ubiquitination, and
458 degradation, similar to that noted in CHIKV infected cells. It is possible that low tolerance for
459 TF in infected or transfected cells results in its sequestration in puncta and ubiquitination; while
460 Scribble is co-localized into the puncta due to its affinity for TF and is degraded simultaneously.
461 Sequestration and ubiquitination of Scribble are not evident in cells transfected with CHIKV 6K,
462 suggesting that TF, and not 6K, is the regulator of the human Scribble protein. TF can be
463 immunoprecipitated with an anti-Scribble antibody from cells infected with WT CHIKV,
464 indicating an association between the two components. Further, a ΔTF version of CHIKV OPY-
465 1 strain generated through reverse genetics, which produces 6K but not TF, cannot trigger
466 Scribble punctation or ubiquitination at the same levels during cellular infection. Infection of
467 cells with the ΔTF variant resulted in substantially enhanced viral RNA load, coupled with
468 reduced infectious particles in the supernatant, indicating that the lack of TF indeed causes
469 disruption in the release and propagation of CHIKV. The punctation and degradation of Scribble
470 by TF is likely essential for modulation of cellular polarity resulting in propagation of the virus.
471 Since TF and 6K share approximately two-thirds of their amino acid sequence, this functional
472 difference is likely to originate from the unique C-terminal region of TF, which contains the PDZ
473 domain binding motif (PBM) as a prominent feature.
474
475 Other viral proteins such as IAV NS1, TBEV NS5, HTLV tax, HCV NS4B and HPV-16 E6 are
476 known to associate with the PDZ domains of Scribble through their PBMs (Javorsky *et al.*, 2023).
477 *In silico* analysis of the unique C-terminus of TF indicated the presence of a Class I PBM which
478 could interact with the PDZ domains of Scribble. Mutational analysis of the predicted PBM
479 confirmed its involvement in regulating Scribble localization. The TF constructs with the PBM
480 mutated were mis-localized, as they were distributed throughout the cytoplasm, and were unable
481 to co-localize with or trigger the sequestration and ubiquitination of Scribble. Mutations in TF
482 PBM also resulted in somewhat decreased protein levels, particularly in the quadruple alanine
483 mutant, which could be due to the drastic nature of the mutation. However, the expressed protein
484 clearly showed an altered localization pattern distinct from wildtype TF. Further, while GFP-TF
485 with an intact PBM could be immunoprecipitated from transfected cells, TF constructs with
486 mutated PBMs could not be pulled down with an anti-Scribble antibody. MS analysis confirmed

487 the weakening of Scribble-TF association upon mutating the TF PBM, which suggests a central
488 role for the PDZ-PBM interaction in this association.
489
490 While transfection of WT TF in HEK293T cells caused mislocalization and ubiquitination of
491 Scribble; the reduction in Scribble protein quantity was marginal compared to the drastic
492 decrease observed during CHIKV infection. This could be because of temporal alterations in TF
493 expression in the transfection versus the infection model, or due to the differences in the quantity
494 of TF production in these cases. The onset of protein detection is usually delayed in transfected
495 compared to infected cells, and it is possible that in HEK293T cells expressing TF,
496 mislocalization and punctation of Scribble precede protein degradation, which occurs at later
497 time points. Also, we found that despite the high transfection efficiency of HEK293T cells, as
498 seen with empty vector producing EGFP, the expression efficiency of EGFP-TF or EGFP-6K by
499 transfection is relatively low, which could be due to the membrane permeabilization capability
500 of these components. It has been shown earlier that expression of 6K in bacterial cells impedes
501 the growth curve significantly, as the membrane activity is likely toxic to the cells (Melton *et al.*,
502 2002; Sanz *et al.*, 1994). Thus, reduced levels of TF expression in transfected HEK293T cells
503 may be a possible reason for decreased levels of Scribble degradation, compared to those
504 observed in CHIKV-infected cells. However, the decline in Scribble protein levels triggered by
505 transfection of EGFP-TF was absent in the case of PBM-mutated TF constructs, which suggests
506 the crucial role of TF PBM in PDZ-domain dependent association with Scribble. TF may have
507 other roles in other aspects of the alphavirus life cycle, such as assembly and/or budding.
508 However, detailed structural and functional analysis of ΔTF CHIKV is needed to understand the
509 contributions of TF to the assembly and budding processes of alphaviruses at the molecular level.
510
511 The PDZ domain-PBM interaction is one of the most abundant modes of protein-protein
512 interaction. The homologues of CHIKV TF from several other alphaviruses also have PBMs in
513 their unique C-terminal tails that can potentially associate with host partners (Supplementary
514 Figure S7). For example, the predicted TF sequences from O'nyong nyong Virus and Igbo-Ora
515 Virus have Class I PBMs at the C-termini that are almost identical to the PBM in CHIKV TF;
516 while TF sequences from Ross River Virus, Mayaro Virus and Semliki Forest Virus are predicted
517 to contain Class II PBMs (Table 3). Two prominent PBMs, in addition to the one at the C-

518 terminus of TF, are predicted in the CHIKV proteome (Table 4). Residues 418-423 in CHIKV
519 glycoprotein E2 are expected to constitute a Class I PBM, while the C-terminus of 6K is predicted
520 to have a Class II PBM. However, we did not note any co-localization of transiently expressed
521 6K with Scribble, therefore it is possible that this PBM may mediate interactions with other host
522 or viral proteins.
523
524 Human Scribble has four PDZ domains, and their association with several viral proteins has been
525 monitored using biophysical methods such as Isothermal Titration Calorimetry (ITC) and X-ray
526 Crystallography (Javorsky *et al.*, 2022a, 2022b). *In vitro*, IAV NS1 binds to all four PDZ domains
527 of Scribble, with PDZ4 being the tightest binder and PDZ1 being the weakest (Javorsky *et al.*,
528 2022b). TBEV NS5 shows strong binding to both PDZ4 and PDZ3 of Scribble (Werme *et al.*,
529 2008; Javorsky *et al.*, 2022a). Interestingly, the NS4B protein of HCV requires interaction with
530 multiple PDZ domains of Scribble for strong binding. Our study establishes that the association
531 between TF and Scribble is driven by PDZ-PBM interaction. Our *in silico* studies suggest that
532 PDZ1 of Scribble has the highest affinity for the PBM in TF, followed by PDZ4. Therefore,
533 either PDZ1 or both PDZ1 and PDZ4 of Scribble may be involved in the association of Scribble
534 with TF. However, existing studies clearly indicate that the structural determinants of PDZ-PBM
535 binding that mediate virus-host interactions are complex and vary significantly even among
536 similar binding pairs. Based on existing studies, it is possible that multiple PDZ motifs from
537 Scribble, or perhaps all four motifs, are required for optimal TF association. (Hu *et al.*, 2016). A
538 detailed *in vitro* biophysical and structural analysis of the CHIKV TF protein with full-length
539 Scribble, as well as the isolated PDZ domains, is essential in order to understand the binding
540 modalities, including minimal requirements for functional association and cooperativity between
541 different PDZ domains. It is to be noted that other host proteins that are part of the Scribble
542 complex, such as Dlg-1, also contain PDZ domains (Barreda *et al.*, 2020). The potential
543 association of alphavirus TF with other components in the Scribble cell polarity module also
544 requires further study. This will lead to a clearer understanding of host responses and viral
545 countermeasures during infection.
546
547

548 **Materials and methods**

549 **Docking and Molecular Dynamics (MD) simulation**

550 Since there is no experimental structure available for CHIKV TF, a structure predicted using the
551 I-TASSER web server (Yang & Zhang, 2015; Zhang, 2008) was utilized for docking. The model
552 with the highest c-score was selected and further refined using the GalaxyRefine web server
553 (Seok *et al.*, 2021; Shin *et al.*, 2014; Ko *et al.*, 2012). The X-ray crystallographic structures of
554 Scribble PDZ domains (1-4, referred to as ScPDZ1, ScPDZ2, ScPDZ3, and ScPDZ4) and
555 mammalian HTRA1 PDZ (HtPDZ) domain were downloaded from the Protein Data Bank (PDB
556 IDs: 5VWC, 1UJU, 7JO7, 4WYT and 2JOA respectively). All structures were energy minimized
557 prior to docking and simulation studies.

558 Protein-protein docking between TF and the PDZ domains of Scribble and HTRA1 was carried
559 out using the ClusPro web server (Desta *et al.*, 2020; Vajda *et al.*, 2017; Kozakov *et al.*, 2017,
560 2013). The binding interface and affinity of each docked complex were analyzed using LigPlot
561 (Wallace *et al.*, 1995). All-atom MD simulation was carried out for each complex in triplicates
562 as described. Briefly, GROMACS (Van Der Spoel *et al.*, 2005) was used to set up and execute
563 the simulations. Each complex was solvated separately using the SPC water model (Mark &
564 Nilsson, 2001) and neutralized using counter-ions. Periodic boundary condition was applied to
565 each system. Energy minimization was executed using the steepest descent algorithm (Gautam,
566 2021). Position-restrained NVT-NPT ensemble equilibrations were carried out for 500 ps and 1
567 ns respectively. Finally, the systems were subjected to unrestrained dynamics for 100 ns. Nose-
568 Hoover (Martyna *et al.*, 1992) and Parrinello-Rehmann (Parrinello & Rahman, 1981) were used
569 for maintaining the temperature (300K) and pressure (1 bar) during simulations. Electrostatics
570 was maintained using Reaction-Field (Tironi *et al.*, 1995) and LINCS (Hess *et al.*, 1997) was
571 used as the constraints algorithm. A time-step of 2 femtoseconds and the Verlet cutoff scheme
572 was applied. All simulations were carried out using the Gromos 54a7 force field. Trajectory
573 analysis was carried out using the built-in GROMACS tools. VMD (Humphrey *et al.*, 1996) and
574 UCSF Chimera (Pettersen *et al.*, 2004) were used as the visualization tools.

575

576 **Molecular Mechanics Poisson-Boltzmann Surface Area (MM-PBSA) analysis**

577 MM-PBSA was utilized to determine the Gibb's free energy (GFE) of protein-protein
578 interactions. The script g_mmpbsa (Kumari *et al.*, 2014) was used for evaluating the GFE of TF

579 and PDZ domains from simulation trajectories. The following equations were used for the
580 analysis
581 $\Delta G\ bind = \Delta G\ complex - (\Delta G\ protein1 + \Delta G\ protein2)$
582 $\Delta GX = \Delta EMM + \Delta G\ solv - T\Delta SMM$
583 $\Delta EMM = \Delta E\ bonded + \Delta E\ nonbonded = \Delta E\ bonded + (\Delta E\ elec + \Delta E\ vdw)$
584 $\Delta G\ solv = \Delta G\ polar + \Delta G\ nonpolar$
585 where $\Delta G\ complex$ = total free energy of protein-protein complex
586 $\Delta G\ protein1$, $\Delta G\ protein2$ = free energies of proteins in solvent
587 ΔGX = free energy for each entity
588 $\Delta E\ MM$ = vacuum potential energy (combined bonded and nonbonded interactions)
589 $\Delta G\ solv$ = solvation free energy [polar ($\Delta G\ polar$), nonpolar ($\Delta G\ nonpolar$)]
590 $T\Delta S$ = entropic contribution of free energy in vacuum. T is temperature and ΔS is entropy
591 respectively.
592 TΔS MM was not included in this study as g_mmpbsa does not calculate entropy (S). Hence, ΔG
593 *bind* was calculated as follows,
594 $\Delta G\ bind = (\Delta E\ elec + \Delta E\ vdw) + (\Delta G\ polar + \Delta G\ SASA)$
595 where, $\Delta G\ SASA = \Delta G\ nonpolar$ since nonpolar solvation energy was calculated based on the
596 SASA model in this study.
597
598 **Cells and plasmids**
599 Human embryonic kidney (HEK) 293T and Vero cells were grown in Dulbecco's modified Eagle
600 medium (DMEM) (Gibco) supplemented with 10 % fetal bovine serum (FBS) (Gibco) and 1 %
601 antibiotic antimycotic solution (Himedia). The cells were maintained at 37 °C with 5 % CO_2. The
602 cDNA sequences of CHIKV 6K and TF (Supplementary Figure S8) were cloned in the pEGFPC1
603 vector (Clontech) to generate fusion proteins tagged with the Enhanced Green Fluorescent
604 Protein (EGFP) at the N-terminus. The ribosomal slippery site UUUUUUA in the 6K cDNA
605 sequence was silently mutated to UUUCCTG to disrupt the consensus ribosomal frameshifting
606 sequence and produce only 6K without affecting its primary structure (Firth *et al.*, 2008). Alanine
607 substitution mutations were carried out to disrupt the PDZ domain binding motif within amino
608 acids 71-74 of TF. Two mutants – a) G73A S74A and b) H71A G72A G73A S74A, were
609 generated using sequential site-directed mutagenesis (Life Technologies) and were confirmed by

610 DNA sequencing (Supplementary Table S2). The ribosomal slippery was silently mutated to
611 UUUCCTG in a similar way using site-directed mutagenesis and HPLC purified primers
612 (Supplementary Table S2) to produce only 6K CHIKV - ΔTF CHIKV construct.
613
614 **CHIKV infection**
615 For all CHIKV infections, HEK293T cells were seeded 24 h prior to infection by CHIKV (strain
616 119067) (Singh *et al.*, 2018) at a MOI of 0.1. CHIKV was added to the cells post phosphate-
617 buffered saline (PBS) washing for adsorption. After 90 min, cells were again washed with PBS,
618 and complete media was added. Post-infection, cells were incubated for 24 - 48 h in normal cell
619 growth conditions.
620 Mutated CHIKV generation: Vero E6 cells were seeded in a 6-well plate to reach 60%
621 confluency. Cells were then transfected with 5µg of CHIKV plasmid (WT CHIKV), and the
622 mutant generated (ΔTF CHIKV) with polyethyleneimine(PEI) in a ratio of 1:5. The cell
623 supernatant was collected 48 hours post-transfection, centrifuged at 2000 rpm for 10 minutes at
624 4°C. The supernatant was carefully removed, aliquoted, and stored at -80°C. For virus
625 propagation, Vero E6 cells were cultured up to 80% confluency in DMEM supplemented with
626 10% FBS. Before infection, cells were incubated in incomplete media for 2-3 hours. Thereafter,
627 cells were infected with 0.01 MOI of CHIKV and observed for maximum cytopathic effect (40-
628 48 hours post-infection). The supernatant was collected and centrifuged at 2,000 for 10 minutes
629 at 4°C to remove cell debris. The virus supernatant was carefully separated without disturbing
630 the cell pellet and stored at -80°C.
631
632 **Western blotting**
633 HEK293T cells infected with CHIKV were washed with PBS and lysed with RIPA lysis buffer
634 supplemented with a protease inhibitor cocktail (ThermoFisher Scientific) as per the
635 manufacturer's protocol. Total protein was quantified using the bicinchoninic acid (BCA) assay,
636 followed by SDS-PAGE and western blotting with a primary antibody against Scribble (1:500,
637 Santa Cruz sc55543), beta-actin (1:1000, Cell signaling Technology 4967), beta-tubulin (1:200,
638 Santa Cruz sc55529), CHIKV E2 (1:3000, The Native antigen company MAB12130-200), and
639 EGFP (1:3000, Bio Bharati BB-AB0065). Densitometric analysis was performed to quantify the

640 protein levels in western blots using the Fiji software as described elsewhere (Schindelin *et al.*,
641 2012; Davarinejad).
642
643 **TF peptide production and generation of specific antibodies**
644 A 15-amino acid peptide corresponding to the C-terminal region of TF was chemically
645 synthesized and coupled to a carrier protein, Keyhole Limpet Hemocyanin (KLH), via the N-
646 terminus (ThermoFisher Scientific). The KLH-TF peptide was dissolved in DMSO and stored at
647 –20ºC until use.
648 Polyclonal sera against TF were raised by immunizing two New Zealand white rabbits, aged 3-4
649 months, with the KLH-TF peptide emulsified in complete/incomplete Freund's adjuvant
650 (CFA/IFA) as per the following protocol. On Day 0 (priming), 1 mg of KLH-TF peptide was
651 emulsified with CFA and injected subcutaneously into the rabbits. Subsequently, four boosts (on
652 Days 21, 42, 63, 84) were given with 300 µg of the peptide emulsified in IFA intramuscularly.
653 Sera were collected two weeks post-immunization from boost 2 onwards and checked for anti-
654 TF antibodies using immunoblotting.
655
656 **Immunoprecipitation**
657 HEK293T cells were infected with CHIKV at an MOI of 0.1. Cell extracts were prepared 24
658 hours post-infection. A polyclonal antibody against Scribble (Invitrogen PA5-54821) was added
659 overnight to precleared cell extracts at 4 °C on a rocker, followed by incubation with protein A/G
660 agarose beads (Santa Cruz sc-2003) for 1 hour at 4 °C with gentle mixing. The beads were washed
661 thrice with lysis buffer (Tris HCl – 20 mM, KCl – 120 mM, EDTA – 0.2 mM, DTT – 1 mM, and
662 protease inhibitor cocktail). Post-washing, the beads were resuspended in SDS-PAGE buffer, and
663 the samples were analyzed in immunoblots with anti-Scribble and anti-TF antibodies.
664
665 **MBP-tagged protein production in bacteria**
666 The cDNA corresponding to the TF and 6K regions of CHIKV were cloned into the pMALc6T
667 vector (New England Biolabs), in conjunction with N-terminal Histidine and Maltose binding
668 protein (MBP) tags, and a TEV protease cleavage site. Recombinant expression of MBP-tagged
669 TF and 6K proteins was induced by the addition of Isopropyl ß-D-1-thiogalactopyranoside in *E.*
670 *coli* Rosetta pLysS cells at 16 °C at an OD 600 of 0.6. The expressed proteins were 2-step purified

671 by Ni-NTA affinity chromatography followed by size exclusion chromatography (SEC) in a
672 buffer containing 25 mM HEPES, 100 mM NaCl, and the detergent n-Dodecyl β-D maltoside
673 (DDM).
674
675 **Confocal microscopy**
676 HEK293T cells were cultured on glass coverslips and infected with CHIKV at an MOI of 0.1.
677 Twenty-four hours post-infection, cells were washed with chilled PBS and fixed with 4%
678 paraformaldehyde (PFA) for 10 min, followed by permeabilization with 0.1 % Triton X-100 in
679 PBS for 5 min and blocked with 5% bovine serum albumin for 60 min. Immunostaining was
680 performed at 4 °C for Scribble, Ubiquitin, and CHIKV proteins using anti-Scribble (1:500,
681 Invitrogen PA5-54821), anti-Ubiquitin (1:300, Santa Cruz sc-8017), anti-E2 (1:500, The Native
682 Antigen Company MAB12130-200), and anti-capsid (1:200, The Native Antigen Company
683 MAB12131-200) antibodies. Post-primary antibody incubation, Alexa fluor-labelled appropriate
684 secondary antibodies were added for 60 min. All washes were carried out using chilled PBS.
685 Nuclei were labelled with DAPI (Invitrogen D1306) for 10 min, and cells were mounted using
686 Prolong Glass Antifade Mountant (Invitrogen P36982). The slides were dried for a few minutes
687 and sealed with nail paint. Imaging was performed on a confocal microscope (Leica TCS SP8)
688 at a magnification of 63X using the oil immersion objective.
689 For transfection of pEGFPC1 constructs, HEK293T cells were seeded and grown at 37°C for 24
690 h, followed by the addition of plasmid DNA in conjunction with lipofectamine2000 (Invitrogen)
691 according to the manufacturer's protocol. Briefly, DNA and lipofectamine (1:3 w/v) were diluted
692 in Opti-MEM (Gibco) and incubated at room temperature (RT) for 20 min. The DNA-
693 lipofectamine complexes were used to replace the cellular growth medium for 5 h. Twenty-four
694 hours post-transfection, cells were washed thrice with PBS, fixed with 4% PFA, and processed
695 as above. Co-localization was estimated as the percentage of qualified double-positive cells
696 relative to the total number of infected or transfected cells as visualized in four distinct fields.
697
698 **Mass spectroscopy**
699 ***Sample Preparation***: 25µg protein sample was first reduced with 5 mM TCEP and subsequently
700 alkylated with 50 mM iodoacetamide. The protein was then digested with Trypsin at a 1:50
701 Trypsin-to-lysate ratio for 16 hours at 37°C. After digestion, the mixture was purified using a

702 C18 silica cartridge and then concentrated by drying in a speed vac. The resulting dried pellet
703 was resuspended in buffer A, which consists of 2% acetonitrile and 0.1% formic acid.
704 ***Mass Spectrometric Analysis of Peptide Mixtures****:* For mass spectrometric analysis, all the
705 experiments were performed on an Easy-nLC-1000 system (Thermo Fisher Scientific) coupled
706 with an Orbitrap Exploris 240 mass spectrometer (Thermo Fisher Scientific) and equipped with
707 a nano electrospray ion source. 1ug of phosphopeptides sample was dissolved in buffer A
708 containing 2% acetonitrile/0.1% formic acid and resolved using Picofrit column (1.8-micron
709 resin, 15cm length). Gradient elution was performed with a 0–38% gradient of buffer B (80%
710 acetonitrile, 0.1% formic acid) at a flow rate of 500nl/min for 96mins, followed by 90% of buffer
711 B for 11 min and finally column equilibration for 3 minutes. Orbitrap Exploris 240 was used to
712 acquire MS spectra under the following conditions: Max IT = 60ms, AGC target = 300%; RF
713 Lens = 70%; R = 60K, mass range = 375−1500. MS2 data was collected using the following
714 conditions: Max IT= 60ms, R= 15K, AGC target 100%. MS/MS data was acquired using a data-
715 dependent top20 method dynamically choosing the most abundant precursor ions from the survey
716 scan, wherein dynamic exclusion was employed for 30s.
717 ***Data Processing:*** Sample was processed and RAW files generated was analyzed with Proteome
718 Discoverer (v2.5) against UniProt reference database. For dual Sequest and Amanda search, the
719 precursor and fragment mass tolerances were set at 10 ppm and 0.02 Da, respectively. The
720 protease used to generate peptides, i.e. enzyme specificity was set for trypsin/P (cleavage at the
721 C terminus of "K/R: unless followed by "P"). Carbamidomethyl on cysteine as fixed modification
722 and oxidation of methionine and N-terminal acetylation were considered as variable
723 modifications for database search. Both peptide spectrum match and protein false discovery rate
724 were set to 0.01 FDR.
725
726 **shRNA mediated knockdown of Scribble**
727 HEK293T cells were seeded and grown at 37 °C for 24 h, and then the Scribble short hairpin
728 RNA (shRNA) containing plasmid DNAs were transfected with lipofectamine 2000 as described
729 earlier. Four different shRNAs were used in different conditions, either alone or in combination,
730 to optimize Scribble knockdown. The effect of the knockdown was analyzed 36 hours post-
731 transfection using western blot analysis and the results were quantified via densitometry. Two
732 conditions, shRNA.C1: AAACCACAAAATAGAGTCT, and shRNA.C2: a combination of

733 AAACCACAAAATAGAGTCT and TGTACAAACATCACTAGTT, produced maximum and
734 consistent knockdown of ~50 %, and were utilized for further studies.
735
736 **MTT assay**
737 Assays with the tetrazolium dye 3-[4, 5-dimethylthiazol-2-yl]-2, 5-diphenyl tetrazolium bromide
738 (MTT) were performed as described in the product's manual (Himedia) with slight modifications.
739 Briefly, 10 µl MTT (5 mg/ml, Himedia) was added to cells, and the formazan crystals were
740 dissolved in dimethyl sulfoxide after 30 min. The absorbance measurements were recorded at
741 570 and 690 nm.
742
743 **Quantitative real-time polymerase chain reaction (qRT-PCR):**
744 CHIKV-infected HEK293T cells were washed with PBS, harvested in Trizol (Takara), and stored
745 at -80 °C. RNA was isolated from the samples as per the manufacturer's protocol, quantitated
746 using nanodrop (Thermo Scientific), and 5 µg RNA was reverse transcribed into cDNA using a
747 cDNA synthesis kit (Takara Bio) as per the manufacturer's instructions. The cDNA was used to
748 analyze human Scribble and CHIKV E1 expression levels by qRT-PCR using gene-specific
749 primers (Supplementary Table S2). PCR reactions were conducted on an ABI 7500 FAST
750 mastercycler, and the relative quantification of gene expression was carried out using the ΔΔCt
751 method with GAPDH as the housekeeping gene.
752
753 **Plaque assay**
754 Vero cells were seeded in a six-well plate in DMEM with 10% FBS (Gibco) and antibiotics
755 (Corning) and incubated for 24 h at 37°C, 5% CO_2. The cell growth media was then replaced
756 with serum-free media, and cells were incubated for 4-6 h. Subsequently, 10-fold dilutions (10^{-5}
757 to 10^{-7}) of the virus-containing culture supernatants of CHIKV-infected HEK293T cells, in
758 serum-free media, were used to replace the cellular growth media. Virus particles in the diluted
759 culture supernatant were allowed to infect Vero cells for 1 h with shaking every 15 min. Post 1
760 h, the cells were washed with PBS, and 3 ml of an overlay mix of 2% low melting agarose in 2X
761 DMEM was added to each well. The agarose was allowed to solidify at 4°C for 15 min, and cells
762 were then incubated at 37°C for 48 h. For plaque visualization, cells were fixed with 10 %
763 formaldehyde for 4-5 h at room temperature and stained with crystal violet for 5 min, followed

764 by washing with tap water. The plate was allowed to dry for a few minutes, and the plaques were
765 counted. The plaque-forming units (PFU) were calculated using the following formula: PFU/ml
766 = (number of plaques x dilution factor)/(inoculum volume). (Modify the plaque assay details to
767 include Sanchi's new data)
768
769 **Acknowledgements:** The work was funded by the Science and Engineering Research Board,
770 Government of India (grant number SPF/2021/000115) and Indian Council of Medical Research
771 (IIRPIG-2024-01-00529). The authors thank the Central Research Facility (CRF) and Sophisticated
772 Analytical & Technical Help Institutes (SATHI) foundation for the confocal microscopy facility. The
773 authors also extend their thanks to Dr. Anjali Kapoor, CRF, IIT Delhi, for her assistance during
774 confocal microscopy imaging. The authors also thank Prof. Manoj Menon, KSBS, IIT Delhi for
775 providing antibodies. RK and PT would also like to acknowledge IIT Delhi for providing fellowship
776 support.
777
778 **Author contributions:** Conceptualization: RK, DD, PT, MB; Methodology: PT, RK, DD, MB;
779 Investigation: RK, PT, DD, YR, SBK, B, SA, SYM, KS; Resources: SB, MB; Writing-original draft:
780 RK, PT, DD, MB; Writing- review & editing: RK, PT, MB; Visualization: RK, PT, MB; Supervision:
781 SB, MB. Project administration: MB; Funding acquisition: MB.
782
783 **Conflict of interest:**
784 The authors declare no conflict of interest.
785

786 **References**

787 Arpin-André C & Mesnard JM (2007) The PDZ domain-binding motif of the human T cell
788 leukemia virus type 1 tax protein induces mislocalization of the tumor suppressor hScrib in
789 T cells. *J Biol Chem* 282: 33132–33141

790 Barreda D, Gutiérrez-González LH, Martínez-Cordero E, Cabello-Gutiérrez C, Chacón-Salinas
791 R & Santos-Mendoza T (2020) The Scribble Complex PDZ Proteins in Immune Cell
792 Polarities. *J Immunol Res* 2020: 5649790

793 Barreda D, Sánchez-Galindo M, López-Flores J, Nava-Castro KE, Bobadilla K, Salgado-Aguayo
794 A & Santos-Mendoza T (2018) PDZ proteins are expressed and regulated in antigen-
795 presenting cells and are targets of influenza A virus. *J Leukoc Biol* 103: 731–738
796 doi:10.1002/JLB.4AB0517-184R

797 Bartholomeeusen K, Daniel M, LaBeaud DA, Gasque P, Peeling RW, Stephenson KE, Ng LFP
798 & Ariën KK (2023) Chikungunya fever. *Nat Rev Dis Prim* 9: 17

799 Bonello TT & Peifer M (2019) Scribble: A master scaffold in polarity, adhesion, synaptogenesis,
800 and proliferation. *J Cell Biol* 218: 742–756

801 Brown R, Wan J & Kielian M (2018) The Alphavirus Exit Pathway: What We Know and What
802 We Wish We Knew. *Viruses* 10: 89

803 Chmielewski D, Schmid MF, Simmons G, Jin J & Chiu W (2022) Chikungunya virus assembly
804 and budding visualized in situ using cryogenic electron tomography. *Nat Microbiol* 7: 1270–
805 1279

806 Davarinejad H Quantifications of Western Blots with ImageJ.

807 Desta IT, Porter KA, Xia B, Kozakov D & Vajda S (2020) Performance and Its Limits in Rigid
808 Body Protein-Protein Docking. *Structure* 28: 1071-1081.e3

809 Dey D, Siddiqui SI, Mamidi P, Ghosh S, Kumar CS, Chattopadhyay S, Ghosh S & Banerjee M
810 (2019) The effect of amantadine on an ion channel protein from Chikungunya virus. *PLoS*
811 *Negl Trop Dis* 13: e0007548

812 Elmasri Z, Negi V, Kuhn RJ & Jose J (2022) Requirement of a functional ion channel for Sindbis
813 virus glycoprotein transport, CPV-II formation, and efficient virus budding. *PLoS Pathog*
814 18: e1010892

815 Firth AE, Chung BYW, Fleeton MN & Atkins JF (2008) Discovery of frameshifting in
816 Alphavirus 6K resolves a 20-year enigma. *Virol J* 5: 108

817 Gautam B (2021) Energy Minimization. In *Homology Molecular Modeling - Perspectives and*
818 *Applications*, Trindade Maia R Maciel de Moraes Filho R & Campos M (eds) IntechOpen
819 Hallengärd D, Kakoulidou M, Lulla A, Kümmerer BM, Johansson DX, Mutso M, Lulla V,
820 Fazakerley JK, Roques P, Le Grand R, et al (2014) Novel Attenuated Chikungunya Vaccine
821 Candidates Elicit Protective Immunity in C57BL/6 mice. *J Virol* 88: 2858–2866
822 Hess B, Bekker H, Berendsen HJC & Fraaije JGEM (1997) LINCS: A linear constraint solver
823 for molecular simulations. *J Comput Chem* 18: 1463–1472
824 Hu B, Li S, Zhang Z, Xie S, Hu Y, Huang X & Zheng Y (2016) HCV NS4B targets Scribble for
825 proteasome-mediated degradation to facilitate cell transformation. *Tumor Biol* 37: 12387–
826 12396
827 Humphrey W, Dalke A & Schulten K (1996) VMD: Visual molecular dynamics. *J Mol Graph*
828 14: 33–38
829 Inada M, Izawa G, Kobayashi W & Ozawa M (2016) 293 cells express both epithelial as well as
830 mesenchymal cell adhesion molecules. Int J Mol Med 37: 1521–1527.
831 Javorsky A, Humbert PO & Kvansakul M (2022a) Molecular basis of Tick Born encephalitis
832 virus NS5 mediated subversion of apico-basal cell polarity signalling. *Biochem J* 479: 1303–
833 1315
834 Javorsky A, Humbert PO & Kvansakul M (2022b) Structural Basis of the Avian Influenza NS1
835 Protein Interactions with the Cell Polarity Regulator Scribble. *Viruses* 14: 583
836 Javorsky A, Humbert PO & Kvansakul M (2023) Viral subversion of the cell polarity regulator
837 Scribble. *Biochem Soc Trans* 51: 415–426
838 Jose J, Snyder JE & Kuhn RJ (2009) A structural and functional perspective of alphavirus
839 replication and assembly. *Future Microbiol* 4: 837–856
840 Kielian M, Chanel-Vos C & Liao M (2010) Alphavirus entry and membrane fusion. *Viruses* 2:
841 796–825
842 Ko J, Park H, Heo L & Seok C (2012) GalaxyWEB server for protein structure prediction and
843 refinement. *Nucleic Acids Res* 40: W294–W297
844 Kozakov D, Beglov D, Bohnuud T, Mottarella SE, Xia B, Hall DR & Vajda S (2013) How good
845 is automated protein docking? *Proteins Struct Funct Bioinforma* 81: 2159–2166
846 Kozakov D, Hall DR, Xia B, Porter KA, Padhorny D, Yueh C, Beglov D & Vajda S (2017) The
847 ClusPro web server for protein–protein docking. *Nat Protoc* 12: 255–278

848 Krishnakumar V & Kannan M (2020) Microbial Pathogenesis: Virus Pathogen–Host
849 Interactions. In *Model Organisms for Microbial Pathogenesis, Biofilm Formation and*
850 *Antimicrobial Drug Discovery*, Siddhardha B Dyavaiah M & Syed A (eds) pp 19–35.
851 Singapore: Springer, Singapore
852 Kumar M, Michael S, Alvarado-Valverde J, McRossed D Sign©száros B, Sámano-Sánchez H,
853 Zeke A, Dobson L, Lazar T, Örd M, Nagpal A, *et al* (2022) The Eukaryotic Linear Motif
854 resource: 2022 release. *Nucleic Acids Res* 50: D497–D508
855 Kumari R, Kumar R & Lynn A (2014) g_mmpbsa —A GROMACS Tool for High-Throughput
856 MM-PBSA Calculations. *J Chem Inf Model* 54: 1951–1962
857 Kundu K & Backofen R (2014) Cluster based prediction of PDZ-peptide interactions. *BMC*
858 *Genomics* 15: S5
859 Kundu K, Mann M, Costa F & Backofen R (2014) MoDPepInt: An interactive web server for
860 prediction of modular domain-peptide interactions. *Bioinformatics* 30: 2668–2669
861 Liu H, Golebiewski L, Dow EC, Krug RM, Javier RT & Rice AP (2010) The ESEV PDZ-Binding
862 Motif of the Avian Influenza A Virus NS1 Protein Protects Infected Cells from Apoptosis
863 by Directly Targeting Scribble. *J Virol* 84: 11164–11174
864 Ma-Lauer Y, Lei J, Hilgenfeld R & von Brunn A (2012) Virus–host interactomes — antiviral
865 drug discovery. *Curr Opin Virol* 2: 614–621
866 Mark P & Nilsson L (2001) Structure and Dynamics of the TIP3P, SPC, and SPC/E Water
867 Models at 298 K. *J Phys Chem A* 105: 9954–9960
868 Martyna GJ, Klein ML & Tuckerman M (1992) Nosé–Hoover chains: The canonical ensemble
869 via continuous dynamics. *J Chem Phys* 97: 2635–2643
870 Melton J V., Ewart GD, Weir RC, Board PG, Lee E & Gage PW (2002) Alphavirus 6K proteins
871 form ion channels. *J Biol Chem* 277: 46923–46931
872 Millsapps EM, Underwood EC & Barr KL (2022) Development and Application of Treatment
873 for Chikungunya Fever. *Res Rep Trop Med* 13: 55–66
874 Nakagawa S & Huibregtse JM (2000) Human Scribble (Vartul) Is Targeted for Ubiquitin-
875 Mediated Degradation by the High-Risk Papillomavirus E6 Proteins and the E6AP
876 Ubiquitin-Protein Ligase. *Mol Cell Biol* 20: 8244–8253
877 Parrinello M & Rahman A (1981) Polymorphic transitions in single crystals: A new molecular
878 dynamics method. *J Appl Phys* 52: 7182–7190

879 Pettersen EF, Goddard TD, Huang CC, Couch GS, Greenblatt DM, Meng EC & Ferrin TE (2004)
880 UCSF Chimera?A visualization system for exploratory research and analysis. *J Comput*
881 *Chem* 25: 1605–1612
882 Ramsey J, Chavez M & Mukhopadhyay S (2019) Domains of the TF protein important in
883 regulating its own palmitoylation. *Virology* 531: 31–39
884 Ramsey J & Mukhopadhyay S (2017) Disentangling the frames, the state of research on the
885 alphavirus 6K and TF proteins. *Viruses* 9: 228
886 Ramsey J, Renzi EC, Arnold RJ, Trinidad JC & Mukhopadhyay S (2017) Palmitoylation of
887 Sindbis Virus TF Protein Regulates Its Plasma Membrane Localization and Subsequent
888 Incorporation into Virions. *J Virol* 91: e02000-16
889 Santoni MJ, Kashyap R, Camoin L & Borg JP (2020) The Scribble family in cancer: twentieth
890 anniversary. *Oncogene* 39: 7019–7033
891 Sanz MA, Pérez L & Carrasco L (1994) Semliki forest virus 6K protein modifies membrane
892 permeability after inducible expression in Escherichia coli cells. *J Biol Chem* 269: 12106–
893 12110
894 Schindelin J, Arganda-Carreras I, Frise E, Kaynig V, Longair M, Pietzsch T, Preibisch S, Rueden
895 C, Saalfeld S, Schmid B, *et al* (2012) Fiji: An open-source platform for biological-image
896 analysis. *Nat Methods* 9: 676–682
897 Seok C, Baek M, Steinegger M, Park H, Lee GR & Won J (2021) Accurate protein structure
898 prediction: what comes next? *BIODESIGN* 9: 47–50
899 Shin W-H, Lee GR, Heo L, Lee H & Seok C (2014) Prediction of Protein Structure and
900 Interaction by GALAXY protein modeling programs. *Bio Des* 2: 1–11
901 Singh H, Mudgal R, Narwal M, Kaur R, Singh VA, Malik A, Chaudhary M & Tomar S (2018)
902 Chikungunya virus inhibition by peptidomimetic inhibitors targeting virus-specific cysteine
903 protease. *Biochimie* 149: 51–61
904 Snyder JE, Kulcsar KA, Schultz KLW, Riley CP, Neary JT, Marr S, Jose J, Griffin DE & Kuhn
905 RJ (2013) Functional Characterization of the Alphavirus TF Protein. *J Virol* 87: 8511–8523
906 Van Der Spoel D, Lindahl E, Hess B, Groenhof G, Mark AE & Berendsen HJC (2005)
907 GROMACS: Fast, flexible, and free. *J Comput Chem* 26: 1701–1718
908 Stephens R, Lim K, Portela M, Kvansakul M, Humbert PO & Richardson HE (2018) The
909 Scribble Cell Polarity Module in the Regulation of Cell Signaling in Tissue Development

910 and Tumorigenesis. *J Mol Biol* 430: 3585–3612
911 Sun S, Xiang Y, Akahata W, Holdaway H, Pal P, Zhang X, Diamond MS, Nabel GJ & Rossmann
912 MG (2013) Structural analyses at pseudo atomic resolution of Chikungunya virus and
913 antibodies show mechanisms of neutralization. *Elife* 2: e00435
914 Thomas M & Banks L (2018) PDZ domain proteins and virus infection: gateways to the cell. *J*
915 *Mol Biol* 430**,** 2896–2911.
916 Tironi IG, Sperb R, Smith PE & van Gunsteren WF (1995) A generalized reaction field method
917 for molecular dynamics simulations. *J Chem Phys* 102: 5451–5459
918 Torres-Flores J & Arias C (2015) Tight Junctions Go Viral! *Viruses* 7: 5145–5154
919 Vajda S, Yueh C, Beglov D, Bohnuud T, Mottarella SE, Xia B, Hall DR & Kozakov D (2017)
920 New additions to the ClusPro server motivated by CAPRI. *Proteins Struct Funct Bioinforma*
921 85: 435–444
922 Wahid B, Ali A, Rafique S & Idrees M (2017) Global expansion of chikungunya virus: mapping
923 the 64-year history. *Int J Infect Dis* 58: 69–76
924 Wallace AC, Laskowski RA & Thornton JM (1995) LIGPLOT: a program to generate schematic
925 diagrams of protein-ligand interactions. *"Protein Eng Des Sel* 8: 127–134
926 Wang Y & Nie G (2021) Overview of human HtrA family proteases and their distinctive
927 physiological roles and unique involvement in diseases, especially cancer and pregnancy
928 complications. *Int J Mol Sci* 22
929 Werme K, Wigerius M & Johansson M (2008) Tick-borne encephalitis virus NS5 associates with
930 membrane protein scribble and impairs interferon-stimulated JAK-STAT signalling. *Cell*
931 *Microbiol* 10: 696–712
932 Wong KZ & Chu JJH (2018) The interplay of viral and host factors in chikungunya virus
933 infection: Targets for antiviral strategies
934 Yang J & Zhang Y (2015) Protein Structure and Function Prediction Using I-TASSER. *Curr*
935 *Protoc Bioinforma* 52: 5.8.1–5.8.15
936 Yap ML, Klose T, Urakami A, Hasan SS, Akahata W & Rossmann MG (2017) Structural studies
937 of Chikungunya virus maturation. *Proc Natl Acad Sci* 114: 13703–13707
938 Ye F & Zhang M (2013) Structures and target recognition modes of PDZ domains: Recurring
939 themes and emerging pictures. *Biochem J* 455: 1–14
940 Zhan L, Rosenberg A, Bergami KC, Yu M, Xuan Z, Jaffe AB, Allred C & Muthuswamy SK

941 (2008) Deregulation of Scribble Promotes Mammary Tumorigenesis and Reveals a Role for
942 Cell Polarity in Carcinoma. *Cell* 135: 865–878
943 Zhang Y (2008) I-TASSER server for protein 3D structure prediction. *BMC Bioinformatics* 9:
944 40
945
946
947

948 **FIGURE LEGENDS**

949 **Figure 1. CHIKV TF as a binding partner for human Scribble.** The CHIKV RNA genome
950 has two open reading frames (ORFs) separated by a junctional region (J). The 5' ORF (ORF 1)
951 codes for four non-structural proteins (nsP1-4). The 3' ORF (ORF 2) codes for 5 structural
952 proteins, namely capsid (C), E3, E2, 6K, and E1. The 6K gene has a ribosomal slippery site which
953 leads to the production of a transframe (TF) protein (Firth *et al.,* 2008) (upper panel, A).
954 Schematic of 6K and TF sequences and the ribosome slip site (F at 48th and L at 49th position)
955 (lower panel, A). Potential PDZ binding motifs (PBMs) present in TF as predicted by different
956 softwares (B). Predicted interactions between TF and Scribble PDZ1, Scribble PDZ4, and
957 HTRA1 (C). RMSF plot for TF interactions with Scribble and HTRA1 (D). Binding of TF C-
958 terminal residues with ScPDZ1(E).

959

960 **Figure 2. Indirect assessment of TF and Scribble association in transfected cells through**
961 **confocal microscopy .** HEK293T cells were transfected with pEGFPC1 vector or pEGFPC1
962 plasmids carrying TF or 6K. Twenty-four hours post-transfection, cells were fixed, and
963 immunostaining was performed for Scribble (red). Inset shows zoomed images of an EGFP-TF
964 expressing cell. Arrowheads indicate Scribble puncta and co-localization with TF (A).
965 Mutational analysis of TF and its effect on Scribble localization (B). Expression levels of TF and
966 TF mutants in HEK293T cells. Twenty-four hours post-transfection, cells were lysed, and 6K
967 and TF expression were analyzed using western blot with anti-GFP antibody (C). L: protein
968 ladder, C1: pEGFPC1 empty vector, TF Mut1: EGFP-TF-HGAATV, TF Mut2: EGFP-TF-
969 AAAATV. Immunoprecipitation (IP) of Scribble using Scribble specific antibody (i) and co-IP
970 of TF-Scribble in transfected cells (C1, TF-WT, TF-Mut1 and TF-Mut2) (D). Fluorescent
971 intensity profiles of the lined areas are displayed alongside the merged image in all cases.

972

973 **Figure 3. Assessment of TF-Scribble association in infected cells.** HEK293T cells were
974 infected with CHIKV at 0.1 MOI. Co-localization of TF-Scribble during infection was analyzed
975 using TF and Scribble specific antibodies at the indicated time points (A), Co-localization;
976 Scribble, E2 and Capsid specific antibodies at the indicated time points (B), Co-localization;
977 Scribble, E2 and TF specific antibodies at the indicated time points (C), Immunoprecipitation
978 (IP) of Scribble using Scribble specific antibody and co-IP of TF-Scribble in infected cells (D).

979 Fluorescent intensity profiles of the lined areas are displayed alongside the merged image in all
980 cases.
981
982 **Figure 4. Effect of CHIKV infection on Scribble localization and expression.** HEK293T cells
983 were infected with CHIKV and Scribble levels were analyzed at 24 and 48 hpi using western blot
984 and quantitated using densitometry (A). Effect of TF on Scribble expression. HEK293T cells
985 were transfected with pEGFPC1-TF and its mutants. Only vector and pEGFPC1-6K were also
986 transfected, and Scribble levels were analyzed 48 h post-transfection using western blot and
987 quantitated using densitometry (B) Immunostaining for Ubiquitin (Ubiq) and Scribble in CHIKV
988 infected HEK293T cells at the indicated time points post-infection(C). Data represent mean ±
989 SEM of two biological replicates. Fluorescent intensity profiles of the lined areas are displayed
990 alongside the merged image in all cases.
991
992 **Figure 5. Effect of TF on Scribble ubiquitination**. HEK293T cells were transfected with
993 pEGFPC1 vector or pEGFPC1 plasmids carrying TF or 6K. Twenty-four hours post-transfection,
994 cells were fixed, and immunostaining was performed for Scribble (red) and Ubiquitin (green).
995 Inset shows a zoomed image of an EGFP-TF expressing cell. Arrowhead(white) indicates EGFP-
996 TF, scribble, and ubiq puncta and colocalization in the merged image (D). HEK293T cells were
997 infected with CHIKV, treated with MG132, and Scribble levels were analyzed at 24 hpi using
998 western blot (E). Data represent mean ± SEM of two biological replicates. Fluorescent intensity
999 profiles of the lined areas are displayed alongside the merged image in all cases.
1000
1001 **Figure 6. Effect of Scribble knockdown on CHIKV infection.** Scrib shRNAs were transfected
1002 into HEK293T cells, and knockdown was confirmed 36 hours post-transfection using western
1003 blot and quantitated using densitometry (A). Scribble knockdown was also confirmed at RNA
1004 level using real-time PCR (B). The effect of Scribble knockdown on cell viability was assessed
1005 using MTT assay (C). Thirty-six hours post-transfection, cells were infected with CHIKV at MOI
1006 of 0.1 for 24 hours. The effect of Scribble knockdown on CHIKV progeny virus was determined
1007 using plaque assay (D) and CHIKV RNA levels using real-time PCR (E). Data represents mean
1008 ± SEM. **, $p \leq 0.01$; ***, $p \leq 0.001$, ns: non-significant (Student's *t*-test).
1009

1010 **Figure 7. ΔTF CHIKV is unable to cause Scribble punctation**. A) The infectivity of WT and
1011 ΔTF CHIKV compared using plaque assay and by measuring respective RNA levels using real-
1012 time PCR B)Immunostaining for ubiquitin and Scribble in CHIKV-infected HEK293T cells 12
1013 hours post-infection and 24 hours post-infection. Fluorescent intensity profiles of the lined areas
1014 are displayed alongside the merged image in all cases. C) Western blot depicting scribble
1015 expression in HEK 293T cells infected with 0.1 MOI WT mcherry CHIKV and ΔTF mcherry
1016 CHIKV at 24 hours post-infection and 36 hours post-infection.
1017
1018

1019 **TABLES**

1020 **Table 1. Binding interface of docked complexes**

System	CHIKV-TF (Hydrogen bonds)	CHIKV-TF (Hydrophobic interactions)
TF-ScPDZ1	Asp68, Glu70, Thr75	Trp11, Trp19, Leu23, Ala27, His71, Gly72, Gly73, Ser74
TF-ScPDZ4	Glu70, His71, Gly72, Thr75	Tyr3, Leu10, Trp11, Ala27, Ile30, Val31, Asn34, Leu38
TF-HtPDZ	Gln15, Asn66, Glu70, His71, Gly73	Leu10, Trp11, Leu20, Ser67, Asp68, Pro69, Gly72

1021

1022 **Table 2. Mass spectrometric analysis of immunoprecipitate using anti-Scribble Ab**

Sample	Accession	Description	Coverage [%]	# Peptides	# PSMs
C1	Q14160	Protein scribble homolog OS=Homo sapiens	58	88	771
	GFP	GFP	-	-	-
TF-WT	Q14160	Protein scribble homolog OS=Homo sapiens	58	87	683
	TF-GFP	TF-GFP WT	54	14	83
TF-MUT1	Q14160	Protein scribble homolog OS=Homo sapiens	*58*	*94*	*721*
	TF-GFP MUT1	TF-GFP MUT1	*28*	*7*	*38*
TF-MUT2	Q14160	Protein scribble homolog OS=Homo sapiens	*57*	*83*	*538*
	TF-GFP MUT2	TF-GFP MUT2	*21*	*6*	*41*

1023

1024

1025 **Table 3. Prediction of PBM in alphavirus TF using the ELM software** (Kumar *et al*, 2022)

Alphavirus	**Region**	**PBM**	**Class**
SINV	65-70	CATDTV	Class_3
ONNV	71-76	HGGSTV	Class_1
UNAV	69-74	HGGISV	Class_2
RRV	70-75	CGGVPV	Class_2
IGBO-ORBA	71-76	HGGSTV	Class_1
MAYV	70-75	PSGIPV	Class_2
SFV	70-75	RGGVPV	Class_2
EEEV	NA		
VEEV	NA		
MIDV	NA		

1026

1027 **Table 4. Prediction of PBM in CHIKV proteins using the ELM software** (Kumar *et al*,
1028 2022)

Protein	**Region**	**PBM**	**Class**
nsP1	NA		
nsP2	NA		
nsP3	NA		
nsP4	NA		
Capsid	NA		
E3	NA		
E2	418-423	VRTTKA	Class_1
6K	56-61	AHTVSA	Class_2
TF	71-76	HGGSTV	Class_1
E1	NA		

1029

A)

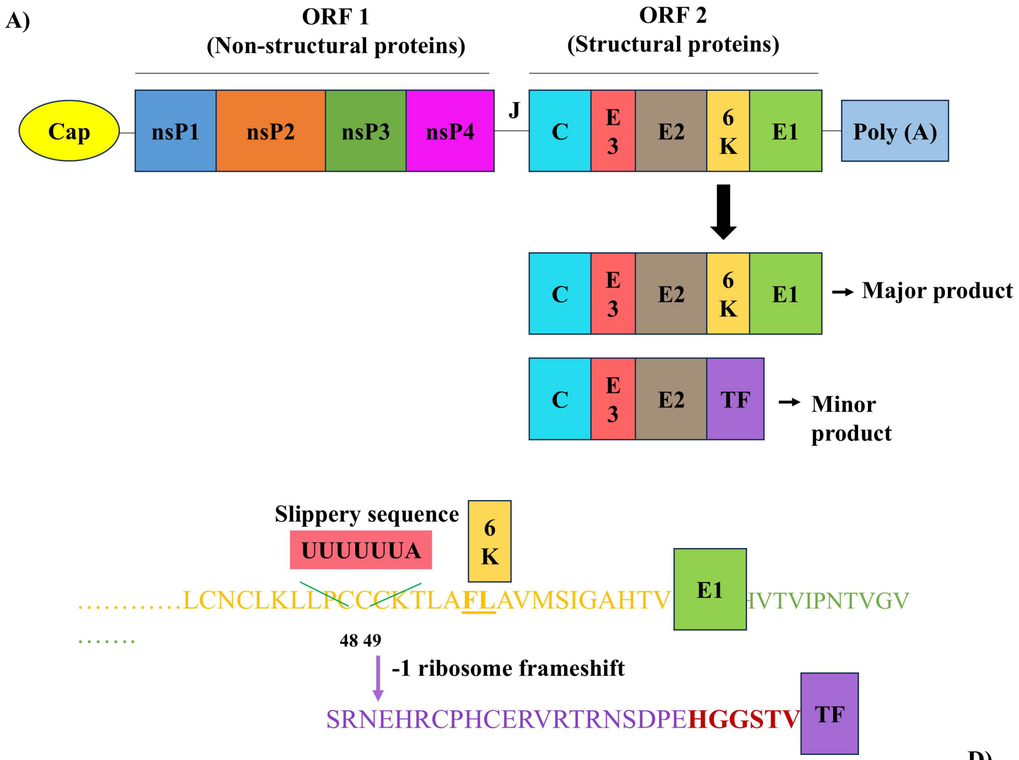

B)

SOFTWARE	REGION	PBM
PDZ PepInt	71-75	HGGST
ELM	71-76	HGGSTV

C)

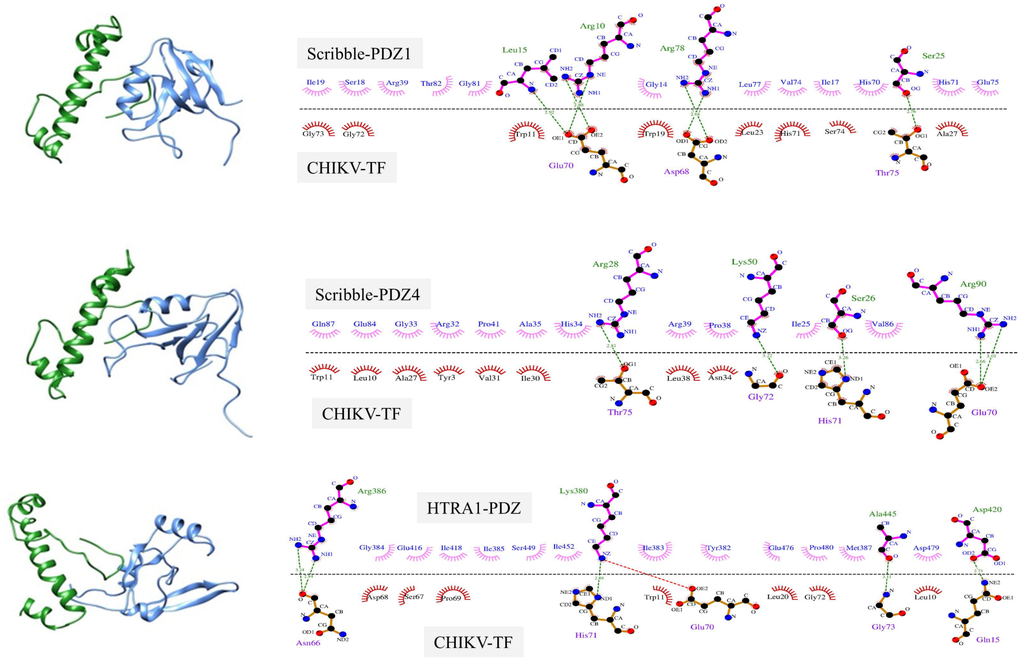

D)

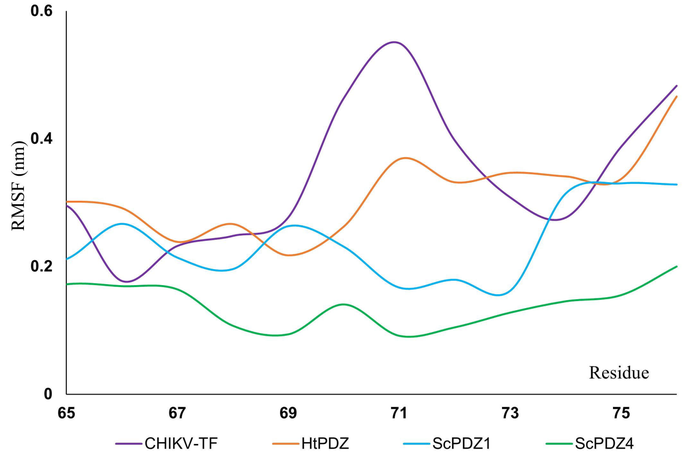

E)

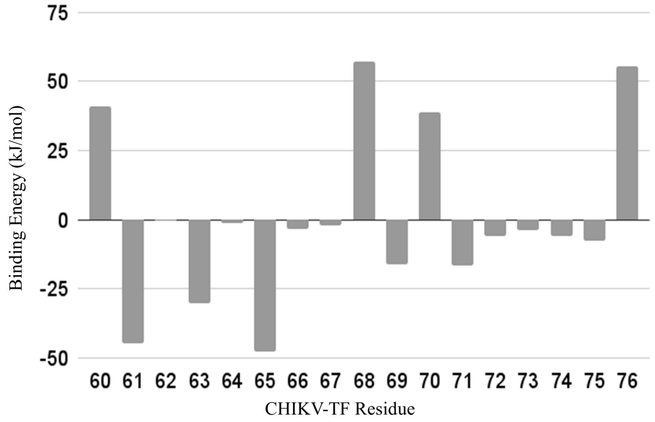

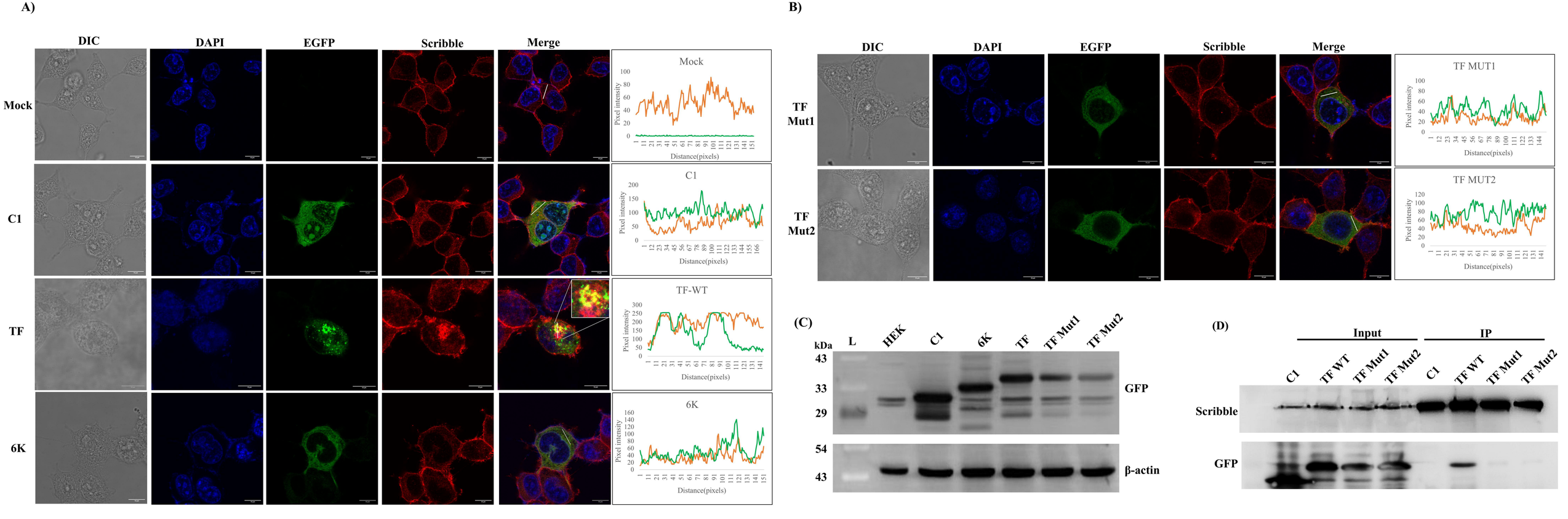
A)
DIC
DAPI
EGFP
Scribble
Merge
Mock
C1
TF
6K
Mock
C1
TF-WT
6K
Pixel intensity
Distance(pixels)
B)
DIC
DAPI
EGFP
Scribble
Merge
TF Mut1
TF Mut2
TF MUT1
TF MUT2
Pixel intensity
Distance(pixels)
(C)
kDa
L
HEK
C1
6K
TF
TF Mut1
TF Mut2
43
33
29
54
43
GFP
β-actin
(D)
Input
IP
C1
TF WT
TF Mut1
TF Mut2
C1
TF WT
TF Mut1
TF Mut2
Scribble
GFP

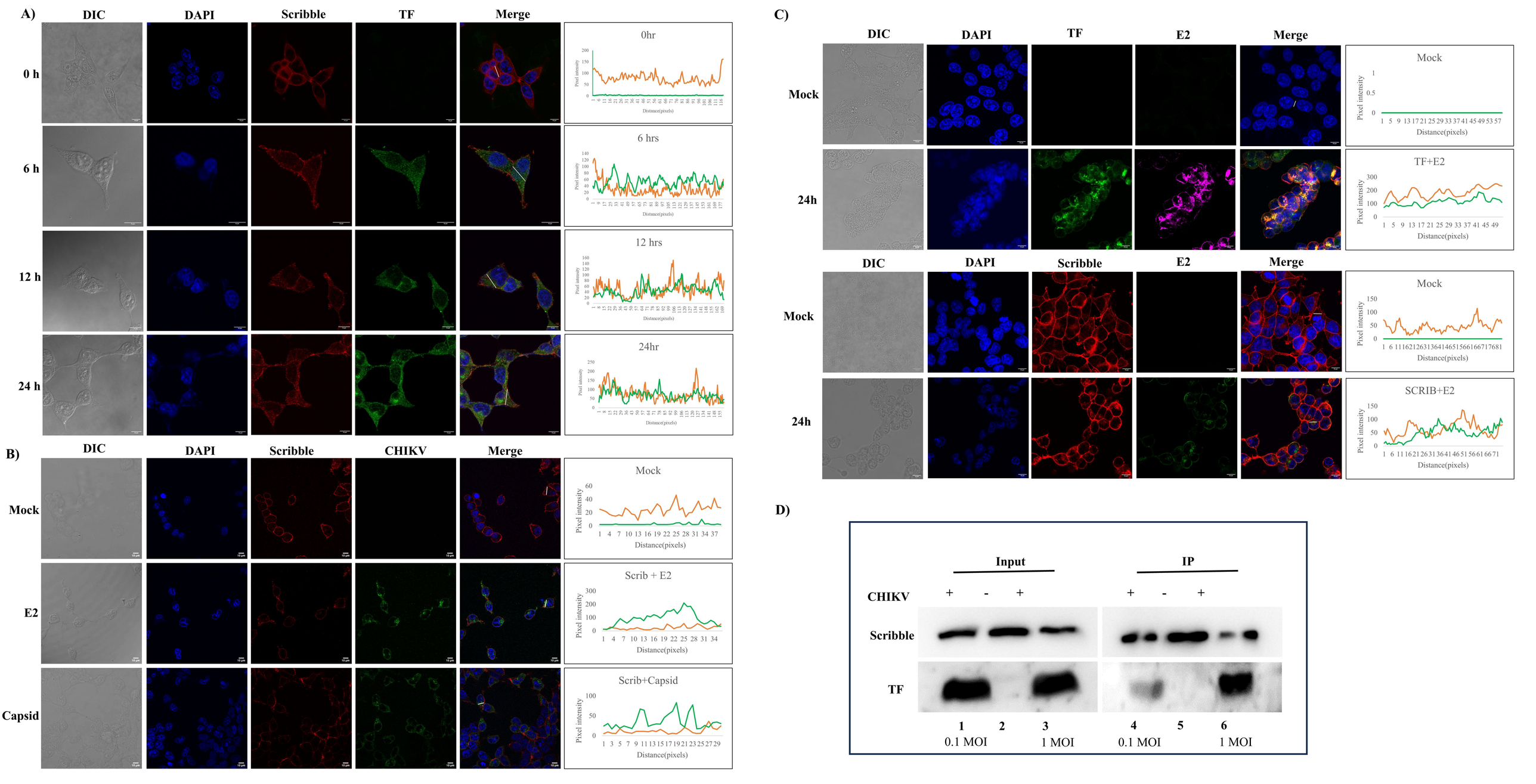
A)
DIC
DAPI
Scribble
TF
Merge
0 h
6 h
12 h
24 h
0hr
6 hrs
12 hrs
24hr
Pixel intensity
Distance(pixels)
B)
DIC
DAPI
Scribble
CHIKV
Merge
Mock
E2
Capsid
Mock
Scrib + E2
Scrib+Capsid
Pixel intensity
Distance(pixels)
C)
DIC
DAPI
TF
E2
Merge
Mock
24h
Mock
TF+E2
DIC
DAPI
Scribble
E2
Merge
Mock
24h
Mock
SCRIB+E2
Pixel intensity
Distance(pixels)
D)
Input
IP
CHIKV
+
-
+
+
-
+
Scribble
TF
1
2
3
4
5
6
0.1 MOI
1 MOI
0.1 MOI
1 MOI

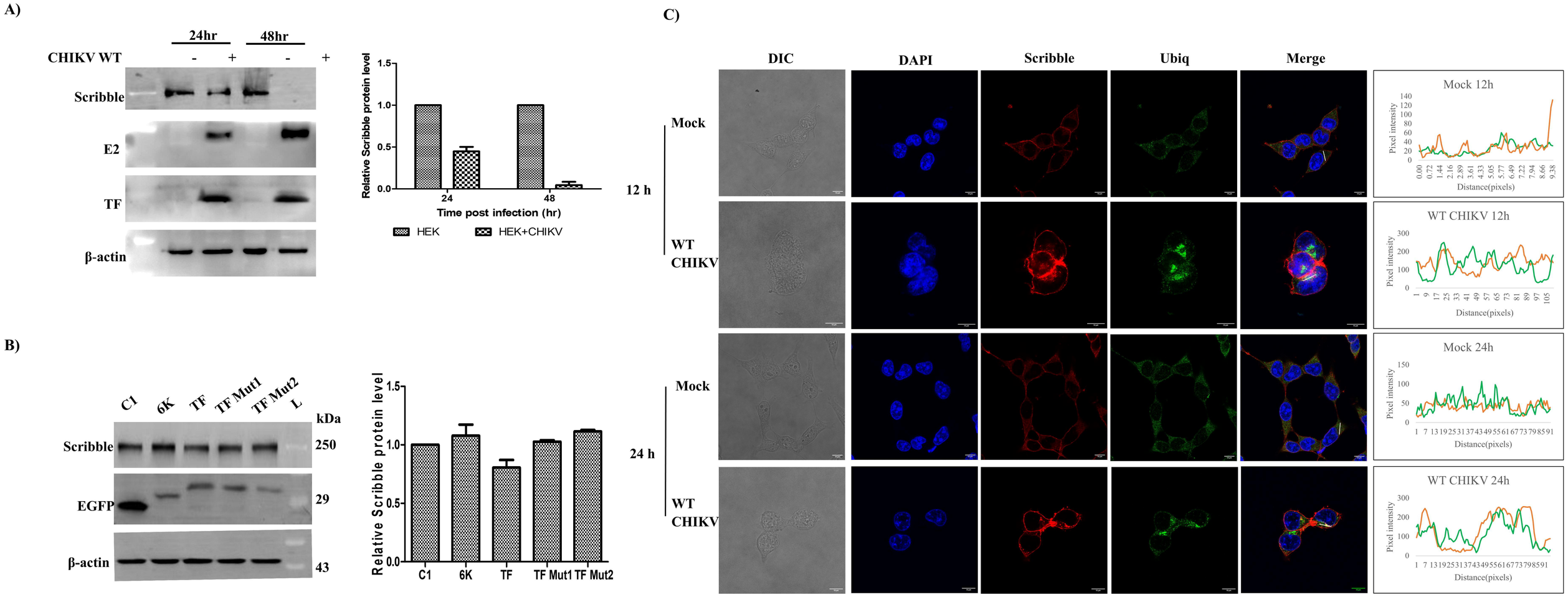
A)
24hr
48hr
CHIKV WT
-
+
-
+
Scribble
E2
TF
β-actin
Relative Scribble protein level
1.5
1.0
0.5
0.0
24
48
Time post infection (hr)
HEK
HEK+CHIKV
B)
C1
6K
TF
TF Mut1
TF Mut2
L
kDa
Scribble
250
EGFP
29
β-actin
43
Relative Scribble protein level
1.5
1.0
0.5
0.0
C1
6K
TF
TF Mut1
TF Mut2
C)
DIC
DAPI
Scribble
Ubiq
Merge
Mock
12 h
WT CHIKV
Mock
24 h
WT CHIKV
Mock 12h
WT CHIKV 12h
Mock 24h
WT CHIKV 24h
Pixel intensity
Distance(pixels)

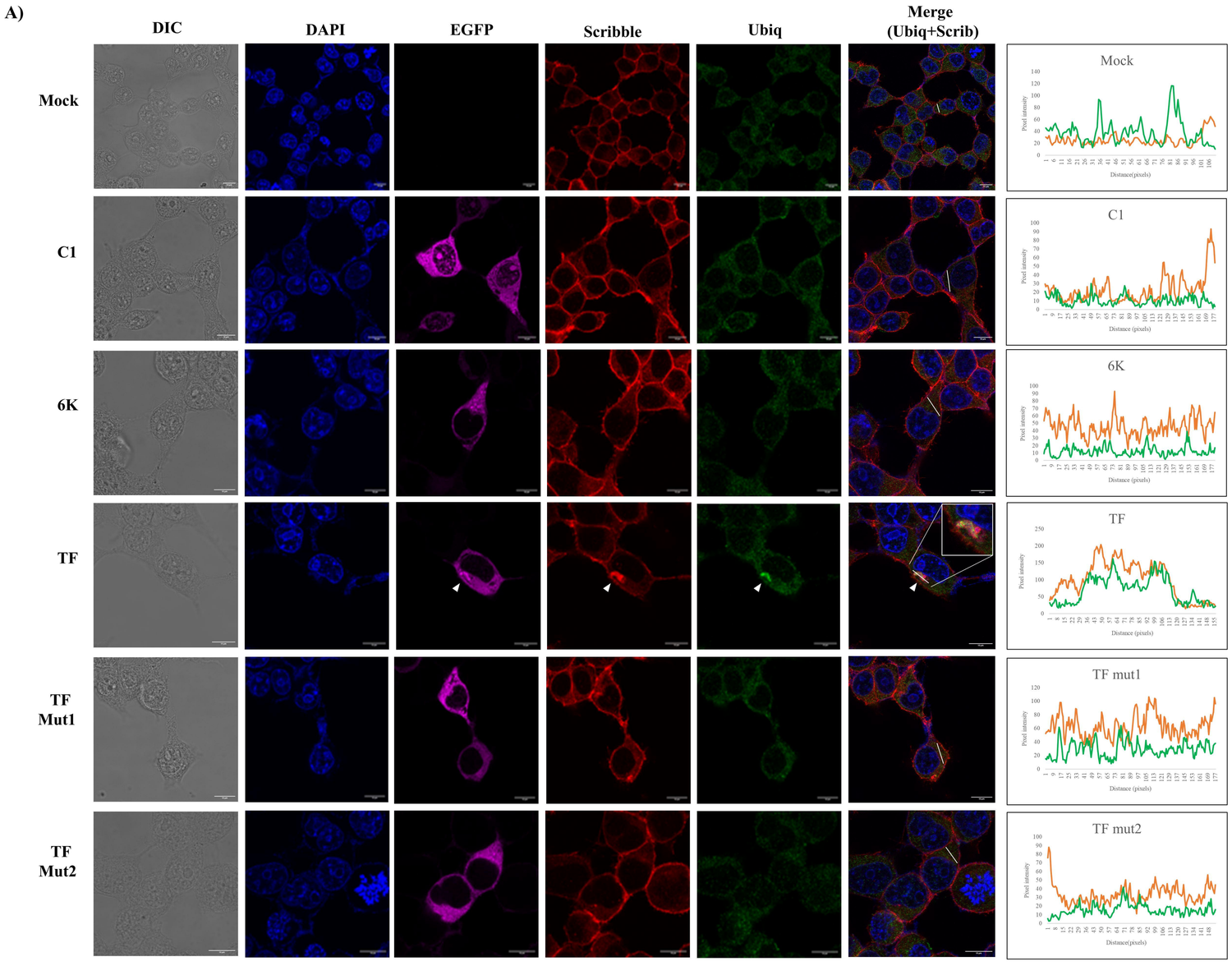
A)
DIC
DAPI
EGFP
Scribble
Ubiq
Merge (Ubiq+Scrib)
Mock
C1
6K
TF
TF Mut1
TF Mut2
Pixel intensity
Distance(pixels)

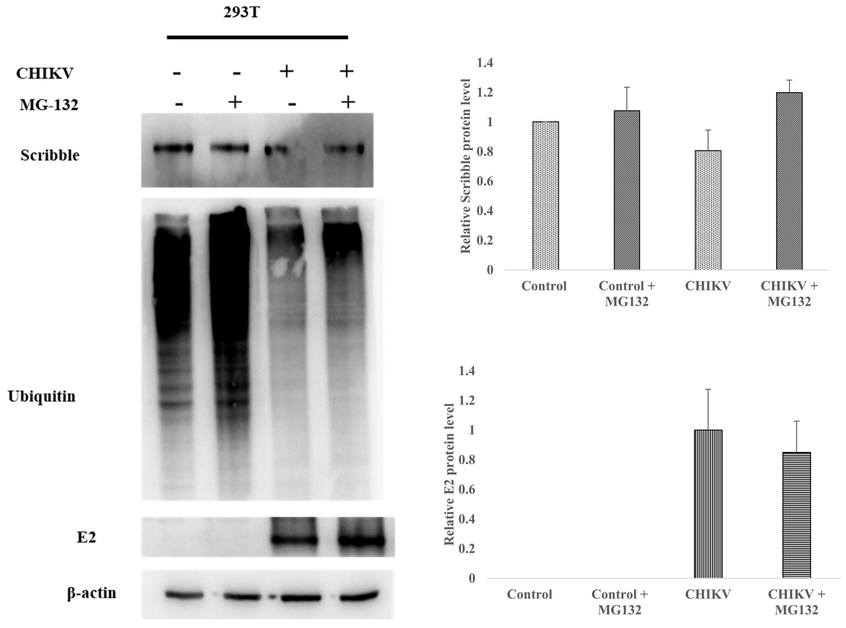
B)
293T
CHIKV
MG-132
Scribble
Ubiquitin
E2
β-actin
Relative Scribble protein level
Relative E2 protein level
Control
Control + MG132
CHIKV
CHIKV + MG132

A)

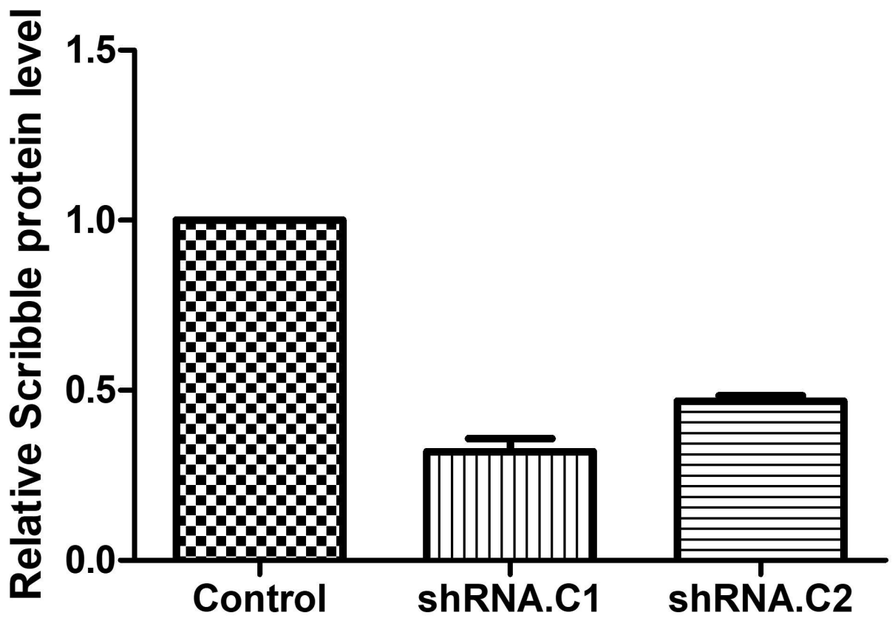
Relative Scribble protein level
1.5
1.0
0.5
0.0
Control
shRNA.C1
shRNA.C2

B)

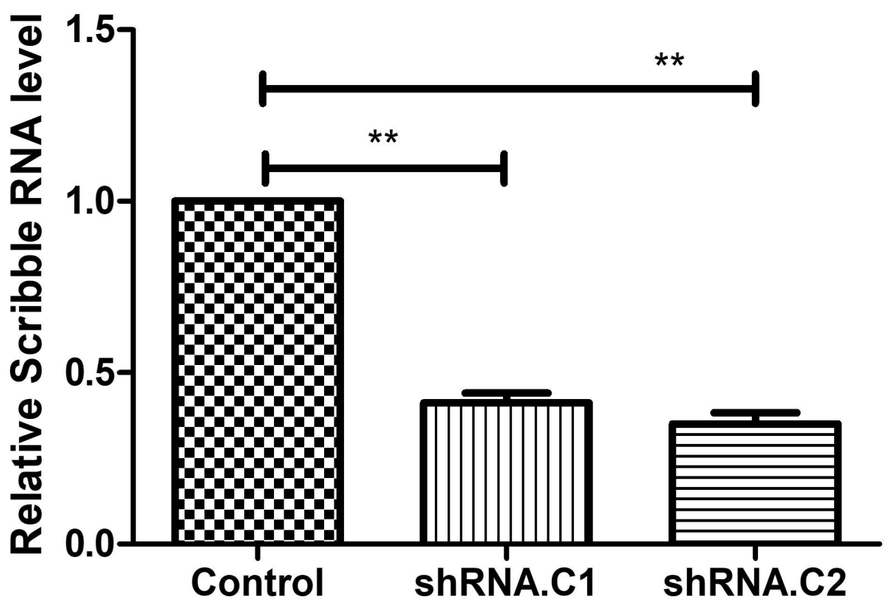
Relative Scribble RNA level
1.5
1.0
0.5
0.0
**
**
Control
shRNA.C1
shRNA.C2

C)

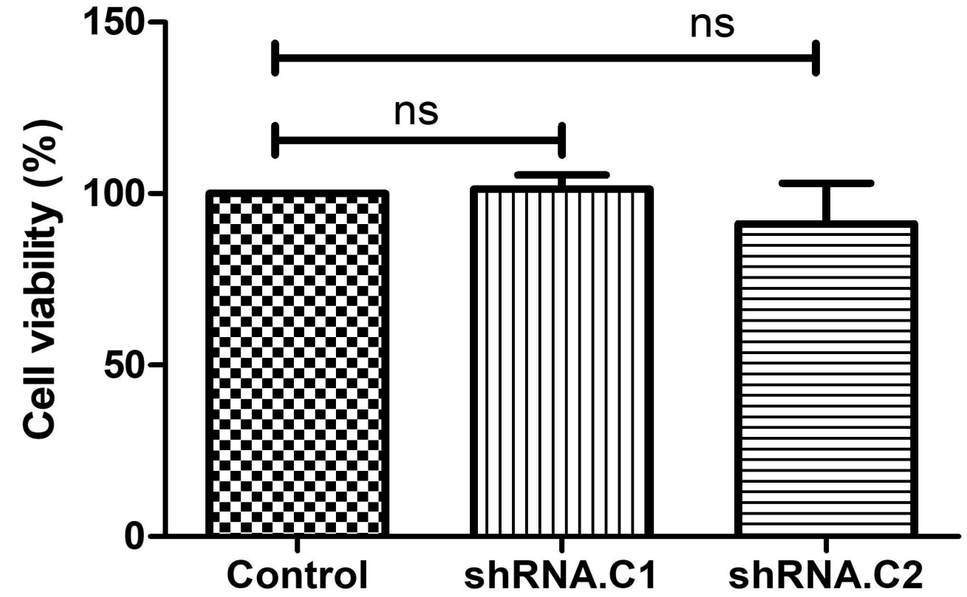
Cell viability (%)
150
100
50
0
ns
ns
Control
shRNA.C1
shRNA.C2

D)

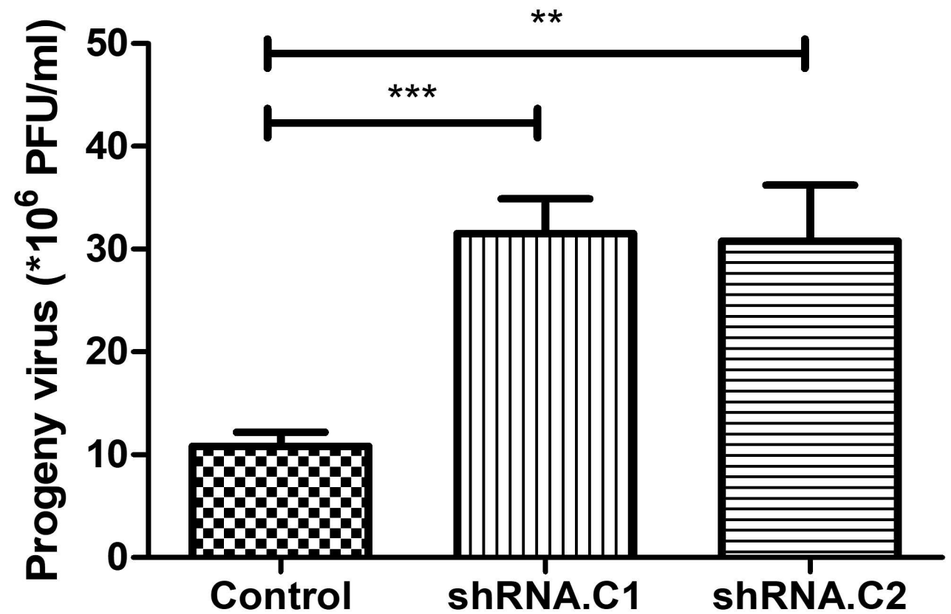
Progeny virus (*10^6 PFU/ml)
50
40
30
20
10
0
**
***
Control
shRNA.C1
shRNA.C2

E)

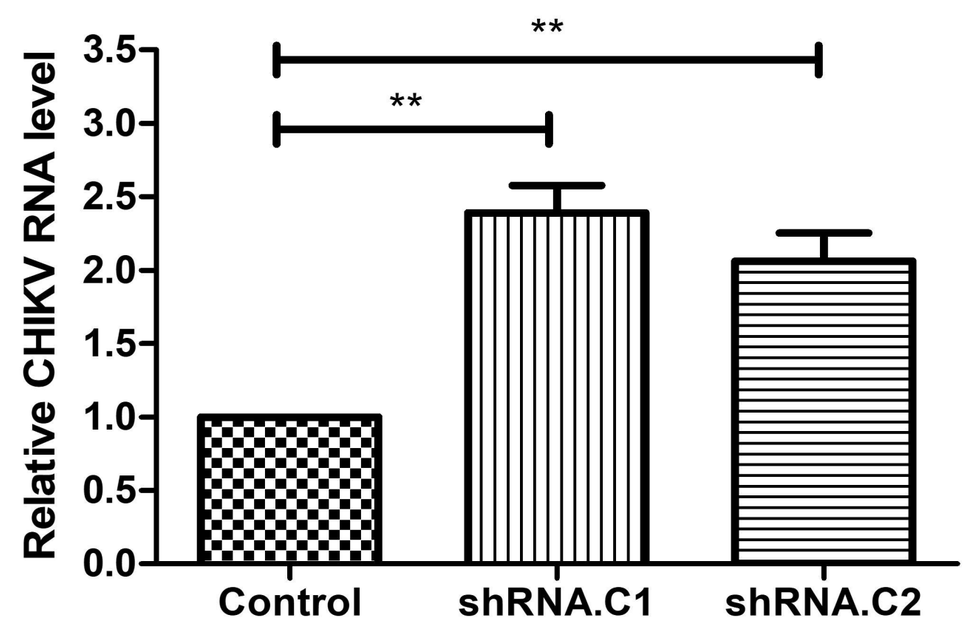
Relative CHIKV RNA level
3.5
3.0
2.5
2.0
1.5
1.0
0.5
0.0
**
**
Control
shRNA.C1
shRNA.C2

A)

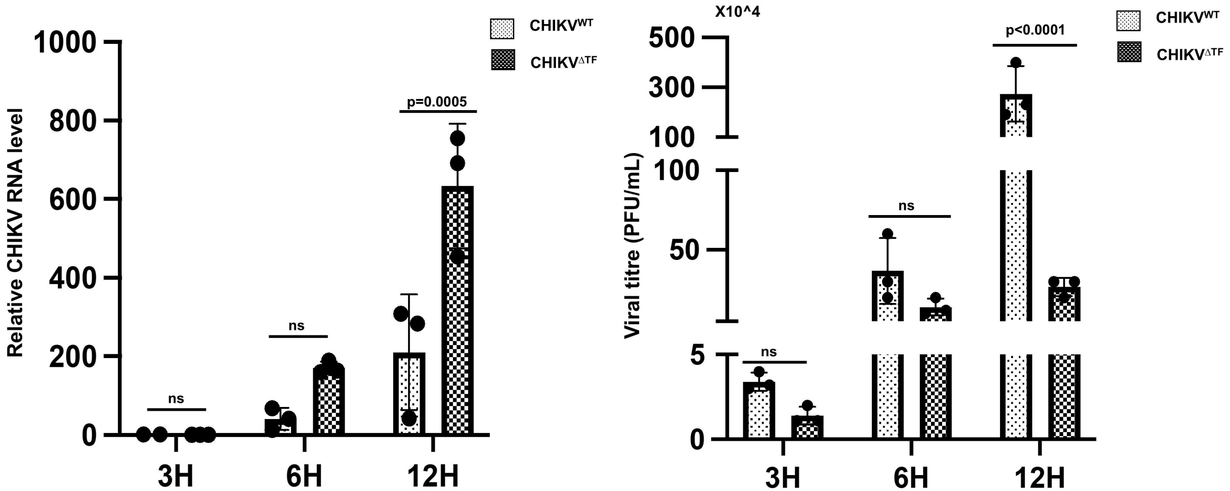
CHIKV^WT
CHIKV^ΔTF
Relative CHIKV RNA level
1000
800
600
400
200
0
ns
ns
p=0.0005
3H
6H
12H
X10^4
500
300
100
100
50
5
0
Viral titre (PFU/mL)
ns
ns
p<0.0001
3H
6H
12H

B)

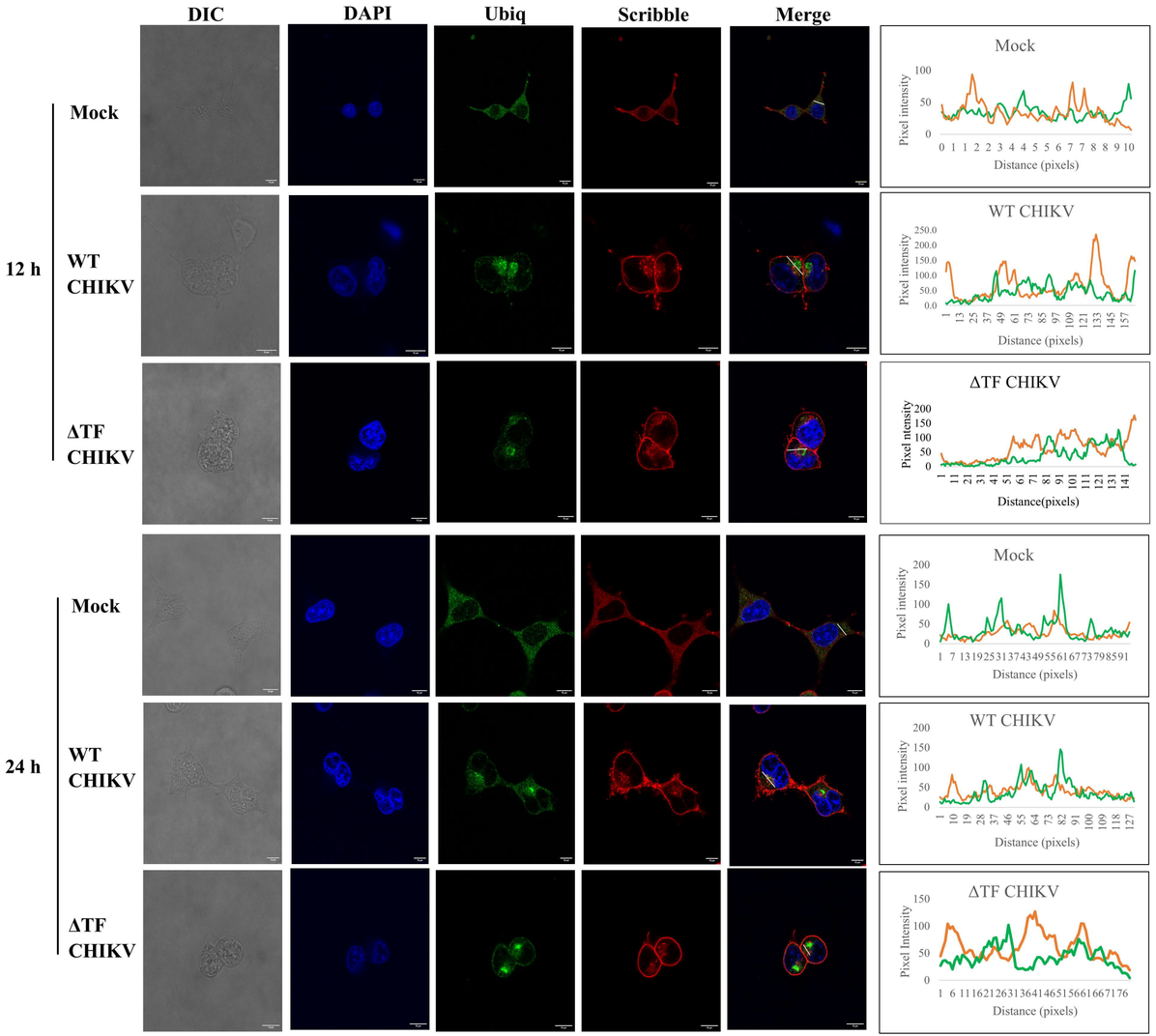
DIC
DAPI
Ubiq
Scribble
Merge
12 h
Mock
WT CHIKV
ΔTF CHIKV
24 h
Mock
WT CHIKV
ΔTF CHIKV
Mock
WT CHIKV
ΔTF CHIKV
Pixel intensity
Distance (pixels)

C)

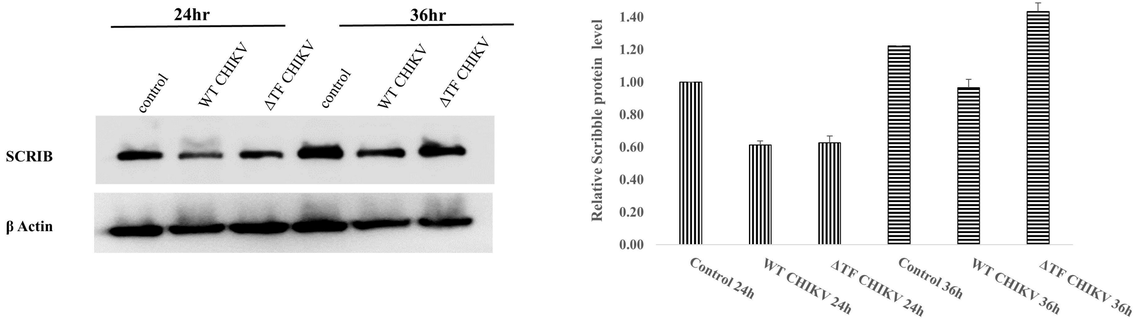
24hr
36hr
control
WT CHIKV
ΔTF CHIKV
control
WT CHIKV
ΔTF CHIKV
SCRIB
β Actin
Relative Scribble protein level
1.60
1.40
1.20
1.00
0.80
0.60
0.40
0.20
0.00
Control 24h
WT CHIKV 24h
ΔTF CHIKV 24h
Control 36h
WT CHIKV 36h
ΔTF CHIKV 36h